Operational strategies for HVDC transmission in smart grids: the security versus markets dilemma

Master Thesis

Chanpreet Kaur Talwar

Technische Universiteit Delft

TU Delft Delft University of Technology

Challenge the future

Operational strategies for HVDC transmission in smart grids: the security versus markets dilemma

Master Thesis

by

Chanpreet Kaur Talwar

in partial fulfillment of the requirements for the degree of

Master of Science

in Electrical Engineering and Computer Science
(Intelligent Electrical Power Grids)

at the Delft University of Technology,

to be defended publicly on Monday August 28, 2017 at 10:00 AM.

Supervisors:	Prof. dr. Peter Palensky,	TU Delft
	Dr. ir. Georgios Papaefthymiou,	Elia Grid International, Germany
	Ir. Martijn de Jong,	TU Delft
Thesis committee:	Prof. dr. Peter Palensky,	TU Delft
	Dr. ir. Jose Luis Rueda Torres,	TU Delft
	Dr. Domenico Lahaye,	TU Delft
	Ir. Martijn de Jong,	TU Delft

An electronic version of this thesis is available at `http://repository.tudelft.nl/`.

TU Delft Delft University of Technology

Preface

First of all, I wish to thank my responsible supervisor, prof. Peter Palensky for guiding me in pursuing my thesis under his kind patronage, and allowing me to be a part of the Intelligent Electrical Power Grid (IEPG) research group in the Netherlands. Second and foremost, I am highly thankful to my daily supervisor Martijn De Jong for his monetary and moral support during the course of thesis studies. Words cannot express my sincere appreciation, but all I can say is that I shall always remain highly obliged and grateful to you for supervising my work, and finding time for me from your busy schedule to clarify all my queries and doubts in the best possible way. I want to thank my supervisor in Germany, George Papaefthimiou for guiding me in pursuing my thesis to this level, and extending valuable suggestions and clarification as and when required.

During the process of study at TU Delft since 2015, I have been receiving constant feedback on my work from Jose Luis Rueda Torres. I wish to thank you for your kind co-operation in helping and guiding me at every stage of the programme with patience and motivation. I would like to extend my gratitude to Domenico Lahaye for being a part of my thesis committee, and for providing me valuable comments on my work .

I wish to thank my dearest parents, Mandeep Singh and Kawaljit Kaur for encouraging me to pursue my quest for further advanced studies out of my mother country. It is because of their support that I could see my dream come true. I would like to thank my best friend, Avik Basu for being with me always. I want to extend my heartiest thanks to my most special friend Bheeshma Chatrath for being my constant pillar of support all through this phase. With his constant encouragement and positivity I have been able to do my best in the thesis. Lastly, I thank my Babaji (my Almighty) for all his beautiful blessings that all my sufferings and disappointments got converted into abundance of happiness and achievements.

Chanpreet Kaur Talwar

Delft, August 2017

Contents

Abstract

Over the last decades, the European transmission system has made many profound changes in the network and has focused on three main concepts: i) flexibility, ii) integration, and iii) sustainability to increase the technological innovations, and to improve the market design. The currently used method by transmission system operators (TSOs) is trying to accomplish these requirements, but it is important to realize that each TSO has its own grid protocols and standards. Consequently, all major TSOs in the interconnected meshed European transmission system are facing a huge difficulty in maintaining a strong operational coordination to work together as a one single European technical market model. In order to guarantee the highest security of electricity supply, it is necessary to structure a stable, reliable and secure analytical AC framework that takes into consideration the stochastic nature of system in-feeds in the daily operational planning. In this thesis it is analyzed how incorporation of smart technologies such as HVDC transmission can be used as a smart grid solution to improve the power system security and lower the risk in different adjacent areas/zones. The proposed risk-based security assessment (RBSA) methodology based on Monte-Carlo sampling is employed to investigate the security of the system and to quantify the expected system risk. It is shown that the market optimal HVDC power set-points may result in unnecessarily high risk when subjected to the unavoidable uncertainty of inputs (fluctuations in load and RES) inherent to day-ahead forecasting. A detailed comparison of market optimal versus security optimal HVDC power set-point is presented. It is proposed to properly adapt the HVDC set-points with respect to the actual operating situation, which can be quite different from the day-ahead point forecast. Moreover, it is shown that by being able to adapt HVDC set-points in real-time operation, further more serious and more costly remedial actions such as active re-dispatch and load shedding, can be avoided. Furthermore, a study with two HVDC transmission lines is performed to show the necessity of coordinated control of the HVDC lines, and how this can reduce the stress in the network by acting as a tool to shift generation.

Keywords: HVDC, set-points, remedial actions, smart grids, RBSA, Monte-Carlo

List of acronyms

AC	Alternating Current
AGC	Automatic Generation Control
CDF	Cumulative Distribution Function
CWE	Central Western Europe
DC	Direct Current
DLF	Deterministic Load Flow
DLR	Dynamic Line Rating
DSM	Demand Side management
DSA	Deterministic Security Assessment
ENTSO-E	European Network of Transmission System Operators for Electricity
EOPF	Enhanced Optimal Power Flow
EU	European Union
FACTS	Flexible Alternating Current Transmission System
FMBC	Flow-based Market Coupling
GISO	Geographically Separated Independent System Operator
GUI	Graphical User Interface
HV	High Voltage
HVAC	High Voltage Alternating Current
HVDC	High Voltage Direct Current
IGBT	Insulated-Gate Bipolar Transistor
LCC	Line Commutated Converter
LV	Low Voltage
MC	Monte-Carlo
MTDC	Multi-terminal Direct Current
MV	Medium Voltage
OHL	Overhead Line
OL-RBSA	Online Risk-based Security assessment
OPF	Optimal Power Flow
PDF	Probability Density Function
PLF	Probabilistic Load Flow
PSA	Probabilistic Security Assessment
PST	Phase Shifting Transformer
PWM	Pulse Width Modulation
RB-DCSA	Risk-based DC Security Assessment

RBSA	Risk-based Security Assessment
RES	Renewable Energy Sources
RSC	Regional Security Coordinator
SOA	System Operation Agreement
SCOPF	Security Constraint Optimal Power Flow
SISO	Super Independent System Operator
SSSC	Static Synchronous Series Compensator
STATCOM	Static Synchronous Compensator
TCSC	Thyristor-Controlled Series Capacitor
TCSR	Thyristor-Controlled Series Reactor
TDP	Time-Dependent Phenomena
TISO	Technology Separated Independent System Operator
TSO	Transmission System Operator
VaS	Value of Security
VRES	Variable Renewable Energy Source
VSC	Voltage Source Converter

List of Figures

List of Tables

To my parents,
Mandeep Singh and Kawaljit Kaur

Chapter 1

Introduction

1.1 Background

The radical transformation of the electrical power industry, along with the growing interest towards smart grid technologies such as power flow controllable components are having a strong impact on the operational security of the European interconnected transmission system. Transition to non-conventional energy sources, decommissioning of conventional power plants, difficulties in constructing new overhead transmission lines (OHLs), incorporation of high voltage direct current (HVDC) transmission systems, implementation of new European network code, and regional market coupling are the several governing factors involved in changing the dynamics of the existing transmission grid infrastructure as illustrated in Figure 1.1 [1, 2, 5, 6]. These radical changes in the existing transmission grid infrastructures moderate the ability of the transmission system operators (TSOs) to assure the highest security of the power system, while maintaining equitably low operating costs. Safeguarding and maintaining the power system security in the existing European transmission system is necessary for successful integration of variable renewable energy sources (VRES) such as wind and solar generation.

The tremendous growth in the share of VRES in the interconnected European transmission system over the last decade has been driven by significant policies set by the European Union (EU). These policies are focused on attaining the EU Energy policy objectives: i) sustainability, ii) security of electricity supply, and iii) competitiveness [1, 2, 7, 8]. However, it must be noted that the successful implementation of the security measures is crucial to support the EU Energy Policy such as, the 20-20-20 targets. The goal is to increase the share of VRES in the transmission system by 20%, mitigate the greenhouse gas emission by 20%, and enhance the energy efficiency by 20% by the year 2020 [1]. Moreover, the attention is deviating towards EU Energy Roadmap 2050, which focuses on reducing the emission of greenhouse gases by 80% by the year 2050 [8]. In May 2015 the establishment of flow-based market coupling (FMBC) has marked a major milestone in the European target electricity model [9] in Central Western Europe (CWE), i.e., the Netherlands, Germany, France, Luxembourg, and Belgium [10]. These emerging policies have a very real impact on the interconnected transmission system whole across Europe. As a result, the European Network of Transmission System Operators for Electricity (ENTSO-E), are exploring solutions on how to overcome the challenges in the changing European interconnected transmission system while maintaining security of power supply.

Large RES penetrating into the meshed network require a power grid upgradability, or an extension to

maintain large energy inflows. In order to overcome the transformation in the existing infrastructure, the VSC-HVDC technology is supposed to be the most suitable solution for the power grid reinforcement and upgradability. It uses pulse width modulation (PWM) control scheme, and provides fast controllability of active and reactive power flows [11]. Hence, the incorporation of VSC-HVDC connections in the European transmission system can facilitate the bulk transmission of electrical power across cross-border electricity market.

As a consequence of these new trends in the European capacity market, the individual TSOs need to assure the security of electricity supply in their domain to facilitate a smooth functioning across cross-border markets. Hence, it is essential to conduct a more comprehensive research on the estimation of the system parameters by incorporating a probabilistic risk-based security assessment (RBSA) framework in the operational day-ahead planning and system operation.

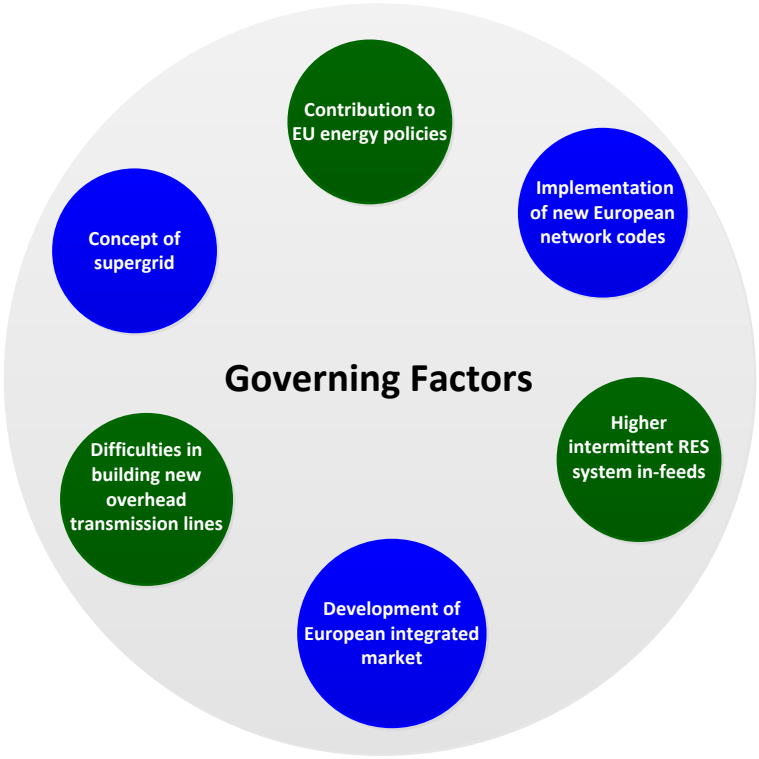

Figure 1.1: Governing factors in the existing transmission grid infrastructure.

1.2 Problem analysis and definition

Many projects based on HVDC technology in the European transmission system are providing eye-catching solutions for exporting bulk amount of electrical power over long transmission distances. The projects based on multi-terminal direct current grids (MTDC) such as DESERTEC and Medgrid, are suggested to integrate massive intermittent renewable energy sources (RES) across Europe, the Middle East and North Africa [11, 12]. These projects are supposed to be the milestones for the European super grid structure. The HVDC installations named Baltic cable, Kontek and SwePol link are established across the Nordic and Central Eastern Europe to relieve the phenomenon of loop flows between Germany, Sweden, Denmark and Poland [13]. The first onshore VSC-HVDC interconnection in Europe is installed between Spain(Vic) and France(Baixas), with a rated transmission capacity of 2GW, and a DC voltage

level of ±320 kilovolts (kV). This onshore VSC-HVDC interconnection is placed in the existing meshed AC synchronous system, and is parallel with the 400 kV Spain(Vic)-France(Baixas) transmission line. In order to manage the flow of DC active power, various control strategies such as i) predefined active power set-points which enables TSOs to fix the active power transfer in the VSC-HVDC connections, and ii) procedures that would emulate the characteristics of the AC transmission line are incorporated [14]. As a result, this transformation in the existing transmission grid infrastructure necessitates the need to analyze how incorporation of HVDC transmission can be used as a smart grid solution to improve power system security and lower the risk in different adjacent areas. Related ideas are discussed under EC FP7 UMBRELLA and iTesla projects, where a risk-based toolbox based on stochastic methods is developed to adequately capture the complex grid operation and help TSOs to access the system risk in the interconnected European transmission system [15, 16].

1.3 Study goals and structure

The integration of stochastic generation and the liberalization of the European energy market poses several operational challenges in a highly meshed European transmission system. In order to guarantee the highest security of electricity supply, it is necessary to structure a stable, reliable and secure analytical AC framework that takes into consideration the stochastic nature of system in-feeds in the daily operational planning. In this thesis it is analyzed how incorporation of an HVDC transmission line can effect the overall system risk, or the risk in different areas/zones. It is shown that HVDC set-points computed by the market may result in unnecessarily high risk. A RBSA methodology using a combination of a Monte-Carlo sampling and the copula theory is employed to quantify the expected system risk in the operational day-ahead planning, taking into account forecast uncertainty and dependence of system in-feeds. It is shown that HVDC set-points should be adjusted in response to the actual operating situation, which can be quite different from the day-ahead point forecast as a result of uncertainty in load and RES in-feeds. It is shown that TSOs cannot always use the cost optimal HVDC set-point computed by the market as there may be cases where the system can run into serious problems. It is shown that by being able to adapt HVDC set-points in real-time operation, further more serious and more costly remedial actions such as active re-dispatch and load shedding, can be avoided. Additionally, a study with two HVDC transmission lines is performed to check how HVDC lines can serve as a tool to shift generation and reduce the stress in the network.

1.4 Research questions

The main research questions for this thesis, addressing *how HVDC transmission can be used as smart grid technology to improve the operational security*, can be formulated as follows:

- ***Investigate how the proposed RBSA methodology can be used in determining the best HVDC set-point when it is subjected to the unavoidable uncertainty of inputs (fluctuations in system in-feeds) inherent to day-ahead forecasting?***

- ***Investigate how the proper adaptability of the HVDC set-points can be ensured in improving the operational security of the interconnected transmission system?***

- ***Investigate how two HVDC transmission lines can work together to find the operating point that provides the best compromise between risk and operating costs?***

1.5 Outline of the thesis

The outline of the thesis is enlisted as follows:

Chapter 2 presents the literature review on power system security, deterministic and probabilistic approaches and smart technologies including HVDC technology, FACTS, DLR and DSM. It gives an account on the power flow modeling, power flow equations, and optimal power flow and its extension.

Chapter 3 discusses the literature on stochastic load and generation. It presents the key aspects on the proposed RBSA methodology used to quantify system risk. It gives an account on how it can be used to assess the system risk in the day-ahead operational planning.

Chapter 4 presents the theory and modeling principles behind HVDC technology. It discusses the current practice concerning day-ahead HVDC operation that are used by TSOs in determining the HVDC set-points.

Chapter 5 present the experimental setup and the several case studies used in analyzing how HVDC transmission line can be used as a smart grid solution to improve power system security. It discusses the results obtained from the study in determining the best HVDC set-point that can achieve the highest security level under all possible uncertainties. It is shown how multiple (two) HVDC lines should be coordinated to provide the best operating point in terms of both security and costs.

Chapter 6 summarizes the main findings of this research and provides the recommendation for the future work.

Figure 1.2 presents the schematic representation of the thesis outline.

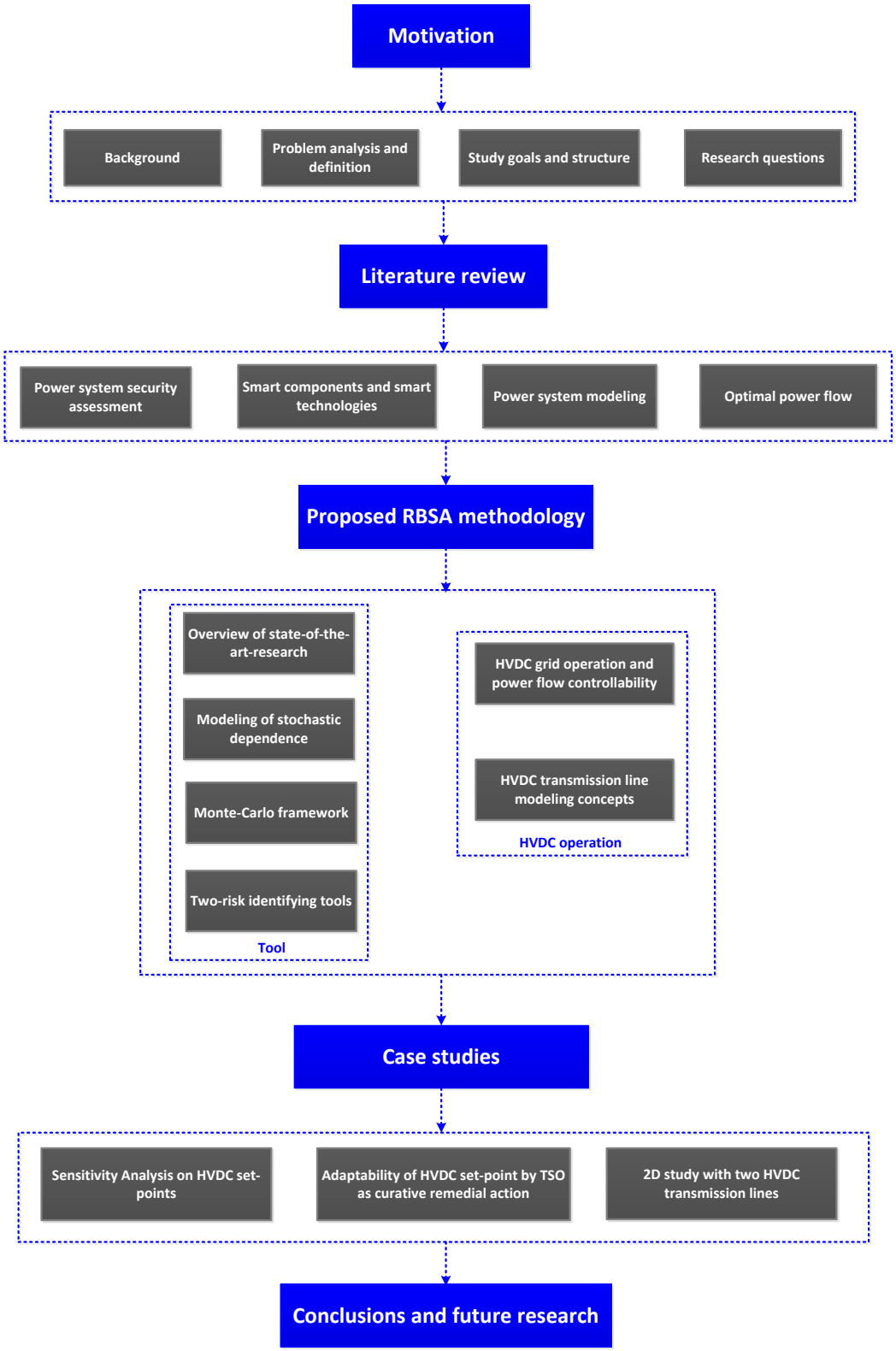

Figure 1.2: Thesis outline.

Chapter 2

Smart grid operation and power flow modeling - a review

2.1 Overview

In this chapter, an overview on the smart grid operation and power flow modeling is presented. A description of power system security assessment is provided in order to understand the need to investigate the expected system risk inherent to day-ahead forecasting. The standard AC (and DC) power flow equations are given, and the need to use optimal power flow to solve the power flow computations is discussed.

2.2 Power system security assessment

Nowaday's power systems are predominantly non-linear and work continuously in varying operating environments. As a result, the operating criteria for a system is to ensure resilience against the most critical as well as non-critical contingencies. Maintaining the security of the system under varying operating environments, and returning the system to an adequate state of security after a disturbance are the main measures taken by TSOs during the power system security assessment. In particular, the decision drivers differentiates between three levels of system security: i) overload security, ii) voltage security, and iii) dynamic security, as illustrated in Figure 2.1 [3]. Many definitions of power system security have been stated over many years. In [17], the security of a power system is stated as:

Security of a power system refers to the degree of risk in its ability to survive imminent disturbances (contingencies) without interruption of customer service. It relates to robustness of the system to imminent disturbances and, hence, depends on the system operating condition as well as the contingent probability of disturbances.

Several operational challenges faced by TSOs are reported in [18], and it states that the high installation of wind in Germany escalates the unscheduled loop flows through German-Czech and German-Polish borders. These unscheduled power flows could exceed the thermal capacities, and can cause severe problems to the entire system. However, in December 2015, a multilateral agreement has been signed between TSOs and ENTSO-e which stated that each TSOs would obtain services by regional security coordinators (RSCs) [4] to improve the power system security. These services are illustrated in Figure 2.2.

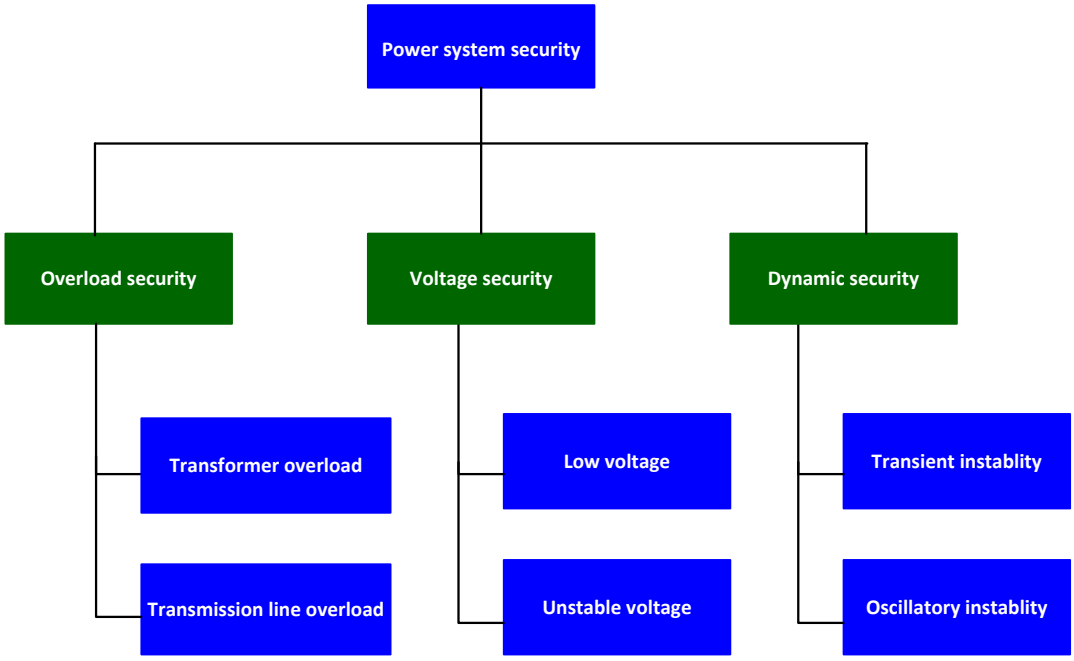

Figure 2.1: Classification of decision drivers of power system security analysis [3].

Hence, the transformation in the existing grid infrastructure necessitates the need to investigate the expected system risk in day-ahead operational planning.

Figure 2.2: Five services to TSOs by RSCs in operational planning for security purposes [4].

To guarantee the overall system security, a balance of economy and quality of power supply should be maintained within certain permissible margins. The security related-decisions are based on different time-periods, which are drawn by system analysts and TSOs to operate and control the power system. Table 2.1 [3] summarizes the time frames on which the security related-decisions are examined. Moreover, the ENTSO-E provides a detailed information on the power system operating states in the Policy 5 of the Emergency Operations handbook [19] in order to assess the bottlenecks in the European transmission system. The classification of the operational security in a power system is described as follows [19]:

- **Normal state:** System state is N-Situation secure and it is within the permissible margin of the allowed operational security. The system has low vulnerability to the critical events such as power balance mismatch, catastrophic failures and power outages;
- **Alert state:** System state is within the permissible margin of the allowed operational security. The system has high vulnerability to the critical events. Remedial curative actions such as re-

Table 2.1: Security related-decisions for TSOs based on different time-periods [3].

Time-period	Decision framer	Security related-decision	Criteria for security related-decision
Real-Time assessment	Operator	How to confine the most economic operation to real-time assessment, maintain the secure operating state?	Operating criteria and cost, real-time rules
Operational planning	Analyst	How the operating criteria should be defined?	Minimal operating criteria and cost, reliability
Seasonal Planning	Analyst	How to upgrade/support the reliability criteria for the network?	Reliability criteria for network plan and cost

dispatching of active power, or re-scheduling of the transmission lines are needed to take the system back to a secure state;

- **Emergency state:** System state has violated the technical operational security limits due to the occurrence of severe disturbances. Emergency control actions are needed to bring the system to the alert state;
- **Blackout state:** System state has violated all the technical operational security limits, and can cause the whole network to collapse;
- **Restorative state:** System state reconnects all the damaged power equipment and re-establishes the connection either to the normal or alert state, and as a result the permissible margin of the allowed operational security is maintained.

The security assessment is associated with the investigation of all possible set of credible as well as non-credible contingencies occurring in the system. The assessment of power system security in day-ahead operation is categorized as follows: i) deterministic security assessment, and ii) probabilistic security assessment [20].

2.2.1 Deterministic security assessment

Deterministic security assessment (DSA) analysis is based on a pre-defined list of the most probable contingencies that may occur in a given system. On occurrence of any probable contingency, the system should operate in such a way that the new operating state is within the post-contingency limits. Thus, the deterministic approach depends on the following two assumptions [20]:

- **Credibility:** the topology of a network, outage of a circuit and operating condition are probable, i.e., they are most likely to happen during the power system security assessment;
- **Severity:** the extent to which the threshold limits of a system are violated. There should not be any probable contingency, wherein the combination of network topology, loss of any component and operation conditions have a more severe effect on the system performance.

The methodology to evaluate for the DSA comprises of the following six steps [20]:

(i) The base cases to represent varied time horizons (years, seasons) and loading levels are selected. The unit commitment is performed for each case based on the selected system topology and time frame;

(ii) The set of credible contingencies based on the (N-1) criterion are considered;

(iii) The study parameters to be investigated are selected, and their ranges of the operating conditions are chosen. This range of operating conditions is called as study range;

(iv) The limiting contingencies, i.e., the events which are first to violate the performance assessment criteria are examined. If there are no violations within the range of the operating conditions, the evaluation is said to be done;

(v) The security boundary is defined by identifying the set of operating condition within the range of operating conditions, i.e., the study range, where a limiting contingency is first to violate the performance assessment criteria;

(vi) The security boundary is then visualized in a form of a sorted table, or plots such that it can be well understood by the operators during the system operation.

2.2.2 Probabilistic security assessment

The DSA methodology is extensively used by TSOs to evaluate the security of the interconnected transmission system. However, there are several weaknesses associated with this methodology, when used to assess the expected system risk: i) only probable contingencies are considered, ii) operating cost is relatively high, and iii) trivial information is obtained about the unacceptable region [21]. Thus, a probabilistic framework is needed in order take into account the contingencies which are rare to occur yet significant in terms of determining the operational security of the system. The probabilistic security assessment (PSA) analysis is based on the set of probable as well as non-probable contingencies to assess the operational risk in a given power system. It takes into account the following aspects: i) uncertainty in load, ii) uncertainty in generation, and iii) uncertainty in contingency. This assessment evaluates the security level by considering, the probability of the event and its severity in one index, named the *risk index* [20, 22].

$$Risk(S) = \sum_{m} P(E_m) * Sev(E_m, S), \tag{2.1}$$

where,

- S is the consequence of the event (e.g., outage of a circuit, load mismatch);
- E_m is the *m-th* event;
- $P(E_m)$ is the probability of the *m-th* event;
- *Sev(E_m, S)* is the severity associated with *m-th* event.

The methodology to evaluate for the PSA comprises of the similar six steps which are discussed in the DSA, however steps 2, 4 and 5 are changed [20]:

(i) The base cases to represent varied time horizons (years, seasons) and loading levels are selected. The unit commitment is performed for each case based on the selected system topology and time frame;

(ii) The set of probable as well as non-probable contingencies are considered, which are based on the procedure of event enumeration. This process is limited by taking into account only those events whose predefined value has been exceeded;

(iii) The study parameters to be investigated are selected, and their ranges of the operating conditions are chosen. This range of operating conditions is termed as study range;

(iv) The risk index is calculated all through the study range, and a threshold level is defined beyond the unacceptable operating condition;

(v) The security boundary is defined by identifying the set of operating condition within the range of operating conditions, i.e., the study range, where the index value is equivalent to the threshold level;

(vi) The security boundary is then visualized in a form of a sorted table, or iso-risk plots such that it can be well understood by the operators during the system operation.

2.3 Review on smart components and smart technologies

The inclusion of smart components such as flexible AC transmission system devices, and high capacity DC interconnectors in the existing energy infrastructure, and the impact of smart technologies such as demand side management and dynamic line rating add capabilities to the power system to handle a broad range of operating points in order to ensure security and reliability. Below an overview is given of the advantages of smart components and smart technologies in the existing grid.

2.3.1 Flexible AC transmission system devices

Flexible AC transmission systems (FACTS) are power electronics-based components, which are used to control power flows or to provide reactive power compensation at weak network points in the AC system [23]. These devices supply the desired amount of reactive power by regulating the bus voltages of the system. Other types of devices such as phase shifting transformers (PSTs) can also be incorporated in the extended range of the FACTS family. These devices can provide active power flow control on the transmission lines by varying the power angle in interconnected electrical systems. FACTS devices are categorized into two groups: i) series compensating elements and, ii) parallel compensating elements. On the one hand, series FACTS compensating elements such as thyristor-controlled series reactor (TCSR), thyristor-controlled series capacitor (TCSC), and static synchronous series compensator (SSSC) can increase the active power flows and henceforth help in controlling the transient stability problems. The TCSC offers a more effective solution for controlling the power oscillation damping of the network, in comparison to parallel FACTS devices. On the other hand, parallel FACTS compensating devices such as static VAR compensator (SVC) and static synchronous compensator (STATCOM) are mainly used to provide voltage support, and regulate the power factor of the network. Such devices provide fast voltage regulation during steady-state and transient instability conditions. They provide fault recovery and can aid in reducing the blackout risk [23].

2.3.2 HVDC technology

Below an overview is given of the advantages of integration of HVDC transmission lines in existing AC grids [24]:

- HVDC connections enable the transmission of bulk power over long distances. For example, the NorNed link is the long distance high-voltage undersea cable of length 580 km connected between Norway and the Netherlands;

- HVDC connections are economical because the line cost is reduced beyond the break-even point. More power per conductor can be transmitted over long distances in a HVDC transmission system. Since only two conductors are required for a bipolar HVDC line, the costs per conductor are lower than for an equivalent AC line;
- HVDC can interconnect two AC asynchronous grids that operate with different nominal frequencies. The HVDC connections can easily adjust to the rated voltage and rated frequency of the system connected at the other end of the network;
- There is no skin effect, and comparatively less line and corona losses in an HVDC transmission system;
- HVDC converters enable bidirectional power flow as they have the ability to operate either in rectification mode or in inversion mode.

The details on HVDC technology are discussed in Chapter 4.

2.3.3 Dynamic line rating (DLR)

The ENTSO-E members are exploring for solutions on how to exploit the existing transmission system infrastructure. The possible solution identified towards the control and planning of such infrastructures, is the implementation of dynamic line rating (DLR) on real-time system operations [25]. The transmission line rating determines the highest current capacity that the transmission line can transfer without violating the static constraints, or jeopardizing system security. However, there exist a crucial difference on how the static and dynamic line rating alleviate congestions and improve the system flexibility. The static line ratings are bounded by the static capacities and computes the static current based on standard atmospheric conditions, while the dynamic line rating computes the dynamic current based on different ambient atmospheric conditions, wind speeds, solar irradiation and precipitation. Therefore, incorporating DLR in the existing system may significantly impact the thermal capacity of the transmission lines which can be used to increase transmission system efficiency of a highly meshed network.

2.3.4 Demand side management (DSM)

Demand side management (DSM) is based on a broad concept where consumers have the capability to modify their usage from their nominal or actual energy consumption patterns by employing various measures such as shifting the consumption to lower tariff periods [26]. Implementing DSM can provide a greater controllability over the electrical power that has been used and produced. Moreover, smart loads such as electric vehicles, energy storage, residential heat pumps, dynamic demand, and other smart applications can further provide flexibility at the consumer side of the network. DSM provides several advantages to the TSOs and further allows for higher incorporation of RES infeed, improved security of power supply and increased network capacity. DSM incentives are divided into four categories: 1) wholesale and balancing markets, 2) grid and retail tariffs, 3) system services and 4) capacity markets. The first two DSM incentives are price triggered, whereas the last two are system integrity triggered. Therefore, DSM is expected to play a vital role in increasing the operational flexibility of the interconnected transmission system.

2.4 Power system modeling

Power flow analysis plays a crucial role in the operational day-ahead planning of the interconnected transmission system [27]. The flow of active power is computed by calculating the angular differ-

ences between the voltages at the buses, whereas the flow of reactive power is computed by calculating the magnitude differences of the voltages at the buses. Moreover, the total active and reactive power injected remains equal to the total active and reactive power extracted, plus the losses along the transmission system. In power flow modeling, the buses are characterized into three types [27]:

- Load buses (PQ buses);
- Generator buses (PV, voltage controlled buses);
- Slack buses (swing buses).

2.5 Power flow equations

2.5.1 DC power flow

The DC power flow problems are formulated by taking into account the following two quantities: i) active power injections and, ii) bus-bar voltage phase angles. In DC power flow modeling, the standard power flow equations are simplified to make the system linear. This linearization of the system reduces the computational time for obtaining the solution. The voltage profiles are approximated to 1 p.u. and all the losses in the transmission system are ignored. The amount of reactive output and bus-bar voltage magnitudes are eliminated, and active power injections result in a linear function of voltage phase angles, and is given by :

$$P_i = \sum_{j=1}^{N} B_{ij}\theta_{ij}, \tag{2.2}$$

where B_{ij} is the susceptance between the bus i and bus j.

The DC power flow computations are fast, and estimate approximate real power flows in the transmission system. Moreover, the assumptions made in the DC power flow equations provide a less accurate power flow solution.

2.5.2 AC power flow

The AC power flow problems are formulated by taking into account the following four quantities: i) active power injections, ii) reactive power injections , iii) bus-bar voltage magnitudes, and iv) bus-bar voltage phase angles. These variables constitute a set of non-linear equations which are linearized and solved iteratively in steps. Following are the standard AC power flow equations for real and reactive power injections:

$$P_i = \sum_{j=1}^{N} |V_i||V_j|(G_{ij}\cos\theta_{ij} + B_{ij}\sin\theta_{ij}), \tag{2.3}$$

$$Q_i = \sum_{j=1}^{N} |V_i||V_j|(G_{ij}\sin\theta_{ij} - B_{ij}\cos\theta_{ij}), \tag{2.4}$$

where P_i and Q_i is the amount of active power and reactive power entering bus-bar i, respectively, and G_{ij} is the conductance between the bus-bar i and bus-bar j.

2.6 Optimal power flow

Mathematically, the AC (and DC) OPF problem formulation is formulated as follows:

Minimize:

$$f(u), \tag{2.5}$$

subject to

$$m(u) = 0, \tag{2.6}$$

$$n(u) \leq 0, \tag{2.7}$$

and

$$u_{min} \leq u \leq u_{max}. \tag{2.8}$$

where *f(u)* is the objective function, and *m(u)*, *n(u)* represent the equality constraints and the inequality constraints respectively. In case of an AC OPF, the optimization vector u represents the active *(P)* and reactive power injections *(Q)*, and bus-bar voltage magnitudes *(V)* and angles *(θ)* [28]. Usually, there are two main objectives in AC OPF which are investigated:

- Total operating cost minimization of active and reactive power output. The summation of cost function can either be a piecewise linear, or a polynomial function:

$$\min \sum_{j=1}^{n_g} f_{cost_j}(P_j) + f_{cost_j}(Q_j), \tag{2.9}$$

  where n_g represents total number of generating units;

- Active power losses minimization of all the branches in the transmission system. The summation of active power losses is given by:

$$\min \sum_{j=1}^{n_l} f_{loss_j}(P_j), \tag{2.10}$$

  where n_l represents total number of branches.

In OPF problem formulation, the constraints are categorized into: i) equality constraints, and ii) inequality constraints. The equality constraints represent the set of power balance equations for active and reactive power output respectively, given by:

$$m_P(\theta, V, P) = 0, \tag{2.11}$$

$$m_Q(\theta, V, Q) = 0. \tag{2.12}$$

The inequality constraints represent the set of operational limits on the branch flows which are expressed in terms of non-linear function of the voltage magnitudes and angles, given by:

$$n_f(\theta, V) \neq 0, \tag{2.13}$$

$$n_t(\theta, V) \neq 0. \tag{2.14}$$

The variable constraints represent the permissible operating ranges for active and reactive injections, and bus voltage magnitudes and angles:

$$P_{min,j} \leq P_j \leq P_{max,j}, \quad \text{where } j = 1 \text{ to } n_g, \tag{2.15}$$

$$Q_{min,j} \leq Q_j \leq Q_{max,j}, \quad \text{where } j = 1 \; to \; n_g, \tag{2.16}$$

$$V_{min,j} \leq V_j \leq V_{max,j}, \quad \text{where } j = 1 \; to \; n_b, \tag{2.17}$$

$$\theta_{ref} \leq \theta_j \leq \theta_{ref} \quad \text{where } j = j_{ref}. \tag{2.18}$$

2.6.1 Need for optimal power flow

The standard power flow problem does not take into account constraints while performing the power flow computation. These constraints include: i) voltage level limits, ii) generation limits, and iii) circuit overloadings. For these reasons, OPF has been developed to properly compute a dispatch that meets all physical constraints, and various objective functions are used commonly, such as: i) reduction of generation costs, and ii) reduction of system losses to obtain a more precise and accurate solution. The proposed RBSA methodology uses AC OPF to perform: i) redispatch active generation, ii) load curtailment, and iii) HVDC remedial action. More details on the RBSA methodology are discussed in Chapter 3.

2.6.2 Extensions of OPF

The standard OPF does not guarantee on how secure the system is against unexpected outages of network elements. In order to be able to compute a feasible generation dispatch that is both cost efficient and also does guarantee that the system is N-1 secure, an extension in OPF is used. This extension in OPF which is used to perform the N-1 contingency analysis is termed as security constraint OPF (SC OPF). The objective is to find cost efficient dispatch, i.e., minimization of active power generation costs such that the dispatch is N-1 secure for all operating conditions. Incorporating SC OPF guarantees a secure grid operation, and makes the system much more reliable [29]. Moreover, an enhanced OPF (EOPF) algorithm with additional constraints for transformer tap ratios, phase shift angles, HVDC transmission lines and shunt elements is proposed under European commission FP7 research project Umbrella [30]. This multi-objective optimization algorithm is efficient enough to synchronize all the possible remedial actions in an optimized way, whilst taking into account all constraints.

An appropriate control strategy is required to guarantee a secure operation of HVDC grids against any unplanned disturbances in the transmission network. The primary control action is carried out by a communication-free scheme such as DC voltage droop control. Secondary control actions are needed for the adaptation of the voltage and active power set-points in response to the uncertainties in loads and RES in-feeds [31, 32]. Usually, an OPF-based tool is used to formulate the secondary control actions for the HVDC grids with various objective functions such as [33]: i) reduction of generation costs, ii) increase of grid security, iii) reduction of system losses, and iv) higher integration of RES. In [34], Iggland and co-workers study the operation of HVAC-HVDC interconnected meshed power systems. They introduce a distributed OPF formulation and propose three operational configurations for interlinked grids: i) the super independent system operator (SISO) where the entire system (both HVAC and HVDC) is controlled centrally by a single entity, ii) the technology separated independent system operator (TISO) where only the HVDC grid is controlled by a separate entity and iii) the geographically separated independent system operator (GISO) where the HVDC and HVAC grids are controlled based on their geographical separation. Thus, it was emphasized that the controllability of HVDC transmission should be incorporated in the OPF formulation in order to compute the cost efficient dispatch in each zone/area.

Chapter 3

Risk-based power system security assessment

3.1 Overview

In this chapter, an overview on modeling of stochastic dependence is presented. A detailed description of the proposed RBSA methodology which is used in [35, 36] is given. It is acknowledged that a risk-based approach should be used by TSOs to quantify the expected system risk in day-ahead security assessment. Moreover, the foundation for the case studies proposed in Chapter 5 on the impact of HVDC power set-points is laid.

3.2 Modeling of stochastic dependence

The massive penetration of stochastic RES, together with the ongoing liberalization of electricity markets have significantly led to higher uncertainties in the operational planning of the European interconnected transmission system. Consequently, this radical change in the existing transmission system has reduced the ability of the TSOs to guarantee the overall security of power supply, while maintaining equitably low operating costs. Uncertainties due to RES in-feeds, and fluctuating loads must be incorporated in the day-ahead planning of the power system. In the next sections, the mathematical concepts of modeling the load forecast uncertainty, renewable generation uncertainty, dependency of the system buses are discussed.

3.2.1 Spatial correlation

The spatial correlation of the snapshot data (point forecasts) should be considered in order to understand the complete representation of the dependence structure of the random variables [37]. The spatial dependency of the snapshot data $X_m (m = 1, ..., n)$ which are assumed to be normally distributed, is described by the product moment correlation matrix C_X.

$$C_X = \begin{bmatrix} \rho^2_{X_1} & \rho_{X_1 X_2} & \cdots & \rho_{X_1 X_n} \\ \rho_{X_2 X_1} & \rho^2_{X_2} & \cdots & \rho_{X_2 X_n} \\ \vdots & \vdots & \ddots & \vdots \\ \rho_{X_n X_1} & \rho_{X_n X_2} & \cdots & \rho^2_{X_n} \end{bmatrix},$$

where ρ stands for Pearson product moment correlation coefficient. By applying Cholesky decomposition, the matrix C_X can be written as [37]:

$$C_X = A \times A^T, \tag{3.1}$$

where A is a lower triangular matrix. The correlated random variables Y are then constructed from the multivariate normal distributions $Z_m(m = 1, ..., n)$ using the matrix C_X [37]:

$$Y = A \times Z_m. \tag{3.2}$$

Lastly, the correlated standard normals are transformed to uniforms by cumulative distribution function (cdf), and by applying the inverse cdf transformation, the correlated uniforms are transformed into the marginals [37].

$$U = \phi(Y), \tag{3.3}$$

$$F = F^{-1}(U). \tag{3.4}$$

3.2.2 Rank correlation

Pearson product moment correlation measures the linear relationship between the random variables. It captures the linear dependence, i.e., when the fluctuation in one random variable is perfectly correlated with the fluctuation in other random variable. This coefficient does not evaluate for the relationships which are not necessarily linear. Therefore, Spearman's rank correlation is used alternatively which allows to measure for all the monotonic relationship between the random variables. It assign ranks to the samples, and then calculates the product moment correlation for the corresponding ranks. The Spearman's rank correlation of random variables $X_m(m = 1, ..., n)$ and $Y_m(m = 1, ..., n)$ with cdfs F_{X_m} and F_{Y_m} is given by [38]:

$$\rho_r(X_m, Y_m) = \rho(F_{X_m}(X_m), F_{Y_m}(Y_m)), \tag{3.5}$$

where ρ_r stands for Spearman's rank correlation.

3.2.3 Copula Theory

In statistical simulation, copula-based function generate multivariate distributions which allow to capture the spatial dependency of the system buses, such as RES and load forecast errors. In particular, copulas can model the non-normal marginals to represent complex stochastic dependency. Abe Sklar in 1959 introduced copulas by describing them as functions that *join together one-dimensional distribution functions to form multivariate distribution functions* [39]. The Sklar's theorem states for every cdf F_{X_m} and F_{Y_m} of random variable $X_m(m = 1, ..., n)$ and $Y_m(m = 1, ..., n)$, there exist a copula such that [38]:

$$F_{X_m Y_m}(x_m, y_m) = C_T(F_{X_m}(x_m), F_{Y_m}(x_m)), \tag{3.6}$$

If all F_{X_m} and F_{Y_m} are continuous, then C_T is unique.

3.3 An overview of state-of-the-art-research

In the recent years, extensive research has been conducted to develop risk-based tools, whilst taking into account forecast uncertainty and dependence of system in-feeds. In [40] Ni, McCalley and co-workers proposed the online risk-based security assessment (OL-RBSA) methodology based on the risk indices to access the security levels of a transmission system with consideration of the possible contingency

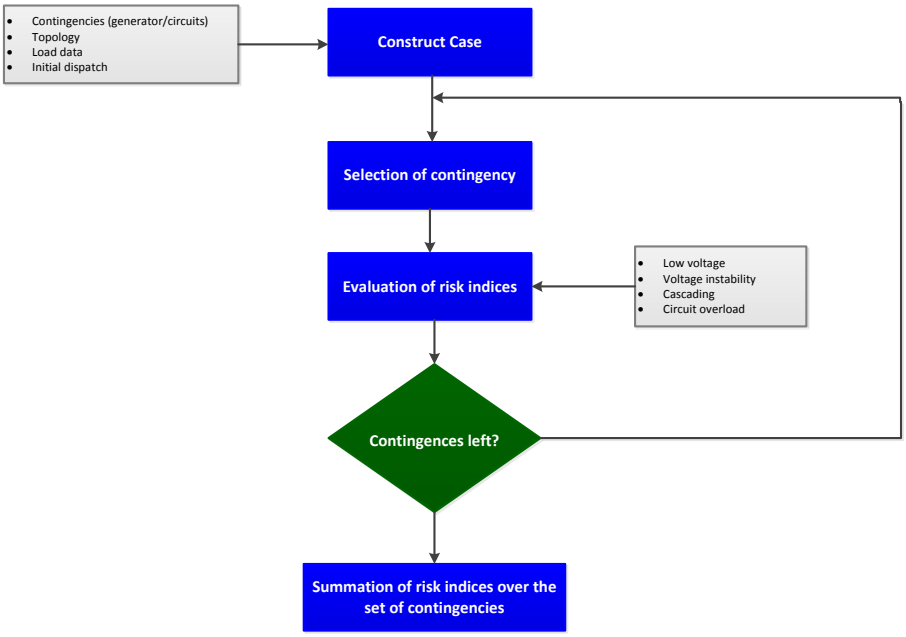

Figure 3.1: Flowchart for McCalley's power system security methodology.

conditions in the near future state. Severity functions are employed to quantify the severity associated with the following: i) low voltage, ii) voltage instability, iii) cascading, and iv) circuit overload. The flowchart for the McCalley's OL-RBSA methodology is illustrated in Figure 3.1, which summarizes the procedure to evaluate for the risk indices using the severity functions.

In [41], Kirschen and co-workers proposed a probabilistic methodology based on MC framework to assess the risk of time-dependent phenomena (TDP), such as transient instability and weather condition, and cascade and sympathetic tripping. This methodology uses MC sampling to evaluate the Value of Security (VaS), which is defined to be the summation of the expected cost of the unscheduled outage, and the cost of the curative measure. The flowchart for the Kirschen's probabilistic methodology for one MC sample is illustrated in Figure 3.2, which summarizes the procedure which is used to calculate VaS in the power system. As can be understood, the McCalley's methodology is based on a pre-defined list of credible contingencies, whereas the Kirschen's probabilistic methodology is based on the set of credible as well as non-credible contingencies to assess the operational risk of the power system.

In [38],[42],[43] Papaefthymiou and co-workers emphasized the importance of copula-function based MC sampling to capture the forecast uncertainty of the system RES inputs inherent to day-ahead forecasting. It has been proposed to use the copula theory which allows for sampling of spatial dependency of the system inputs, and non-Gaussian distributions. It is analysed that the system can run into serious problems when the spatial dependencies of the RES inputs are not taken into consideration. In [44], Longatt and co-workers proposed a risk-based DC security assessment (RB-DCSA) methodology to ensure the security of supply in a highly stressed DC transmission system. Severity functions are employed to quantify the severity associated with the following: i) DC- voltage excursion, ii) cable overload, and iii) converter overload. The methodology takes into account the systemic and individual component risk through a combination of MC sampling and fuzzy interface system. In [45], Li and fellow workers proposed a methodology to study the transmission line overload in wind-power systems using the mathematical concept of severity functions, whilst taking into consideration wind and load-power generation correlation. Moreover, commercial probabilistic planning tools such as GridView, REMARK, PROCOSE,

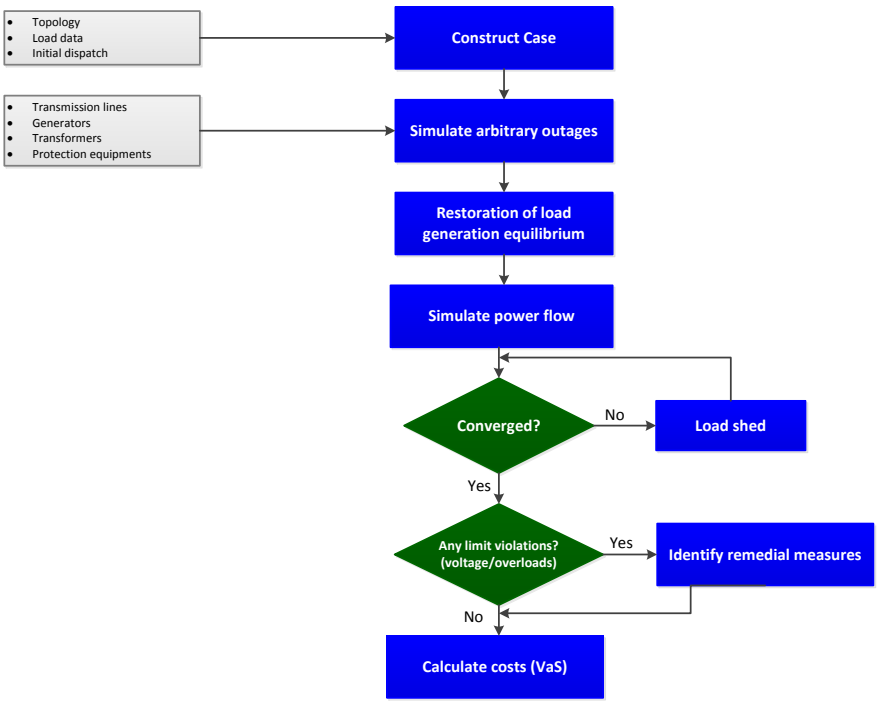

Figure 3.2: Flowchart for Kirschen's probabilistic framework for one MC sample.

CREAM, and CORAL are based on DC PF computations, and may indeed perform poorly if voltage problems are a prime contributor to system risk [46].

In contrast with the other existing methods, the proposed RBSA methodology uses AC and AC OPF combinations to perform a detailed risk assessment in day-ahead operation. The methodology employs a more comprehensive analysis based on AC OPF for alert and emergency situations, which can allow TSOs to steer the system to secure states by providing valuable information on expected curative measures. These key features of the proposed methodology allow for a accurate and complete risk assessment by TSOs. More details on the proposed RBSA methodology are discussed in Section 3.4.

3.4 General overview: Proposed RBSA methodology

In this work the proposed RBSA methodology as presented in [35, 36] is employed to quantify the expected system risk in day-ahead security assessment. The methodology allows to forecast the risk that comes with a provided market dispatch for a day-ahead time horizon. The methodology involves modeling of the random behavior of fluctuating loads and RES in-feeds. The methodology takes into account load and RES forecast errors and spatial dependency of the system in-feeds through a combination of a Monte-Carlo (MC) framework and copula theory. Moreover, the methodology uses full AC PF and AC OPF combinations to obtain a very high level of accuracy in the day-ahead operational planning. The methodology keeps track of the violation of acceptable system limits under a variety of circumstances such as shortage of active generation, voltage violations and thermal branch overloads. Also, the tool can simulate cascading events and it can be used to perform N-1 contingency analysis.

The risk for overloaded circuits, bus voltage deviations, lost loads and cascading events can be evaluated. For this, the methodology employs two tools: i) a fast-screening tool using the concept of

severity functions, and ii) a comprehensive analysis tool using extended AC OPF which provides the valuable information on remedial actions. The proposed remedial actions can help TSOs to steer the system to secure states under all possible uncertainties. There are several graphical display functions included which can be used to visualize the results in a transparent manner, i.e., a GUI to generate color risk-snapshots of the system displaying the regions of highest system stress on a nodal level, iso-risk plots for 2D study parameter studies, and empirical pdfs/cdfs. The layout of the proposed RBSA methodology is illustrated in Figure 3.3.

Figure 3.3: Layout of proposed RBSA methodology.

3.4.1 Monte-Carlo framework

The outline of the proposed RBSA methodology is presented in Figure 3.4. Sample generation in MC framework captures the complex stochasticity of probabilistic forecast of the random variables. The methodology weighs the severity of the risk-based events that are related to outages, blackouts and cascadings with the probability that it would occur in the near future. On the one hand, the severity is related to the overall reliability parameters and violation in the threshold technical limits of the power system. On the other hand, the probability of an event (e.g. voltage exceeding 1.05 p.u.) is evaluated by simple enumeration, i.e., it equals the number of times the event happens divided by the total number of MC samples.

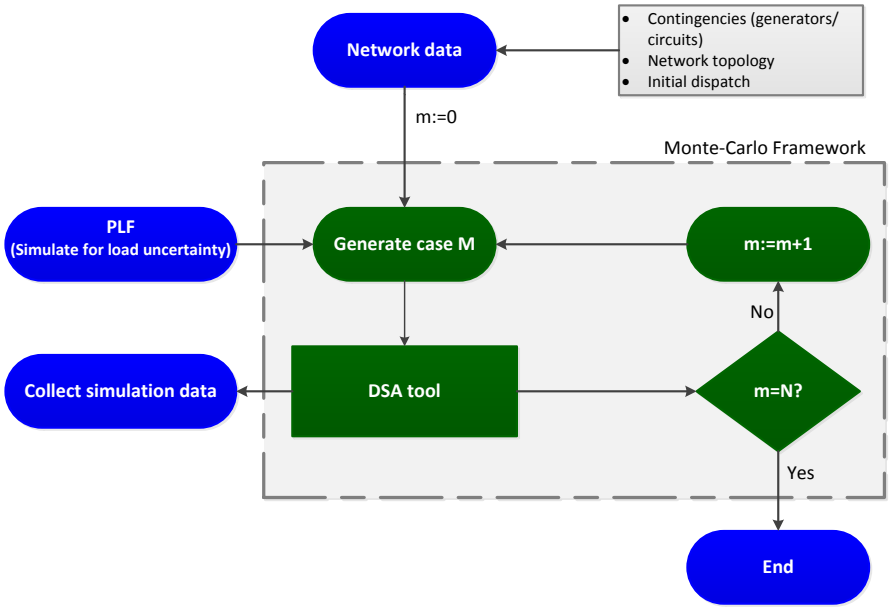

Figure 3.4: Outline of RBSA methodology.

3.4.1.1 Probabilistic load flow (PLF)

The proposed methodology uses copula-function based MC sampling to create a probabilistic load flow (PLF) which captures the forecast uncertainty of the system inputs. For the numerical experiments, the snapshot data i.e., point forecasts are in this work assumed to be normally distributed, but it must be noted that the RBSA methodology can work with modeling of correlated non-normal distributions as well, and empirical distributions by sampling from actual measurements. Here, the point forecast at every bus $m = 1, ..., n_b$ is replaced by a normal marginal, given by:

$$P_m \sim N(\mu_m, \sigma_m), \tag{3.7}$$

where P_m is the active load at bus m, μ_m is mean of the active load and σ_m is the magnitude of the standard deviation chosen to capture the load and RES forecast uncertainty. The reactive load Q_m is computed consequently, by assuming a constant power factor. It must be noted that if the ratio Q_m/P_m is chosen to be constant, then the power factor remains constant. The stochastic dependence between the system buses is described by computing the correlation matrix C. Zone-wise uniform correlation of the active loads is considered to understand the complete representation of the dependence structure of the random variables. Thus, the correlation matrix C of the power system having total number of m buses is given by:

$$C = \begin{bmatrix} C_1 & 0 & 0 & \dots & 0 \\ 0 & C_2 & 0 & \dots & 0 \\ \vdots & \vdots & \vdots & \ddots & \vdots \\ 0 & 0 & 0 & \dots & C_z \end{bmatrix},$$

where the sub-matrix R_z is the uniform correlation matrix for all the buses that are clustered in one zone and is given by:

$$C_z = \begin{bmatrix} 1 & \rho_r & \rho_r & \dots & \rho_r \\ \rho_r & 1 & \rho_r & \dots & \rho_r \\ \vdots & \vdots & \vdots & \ddots & \vdots \\ \rho_r & \rho_r & \rho_r & \dots & 1 \end{bmatrix},$$

where ρ_r represents the rank correlation.

The MC sampling of the random variables are performed based on the copula-based model, where the obtained sample values correspond to the marginal distributions and the correlation matrix C. The ranks of the correlated random variables $U_m(i = 1, ..., n)$, are then constructed from the multivariate normal distributions using the matrix C and the Gaussion copula model. Further, by applying the inverse cdf transformation, the correlated ranks U_m are transformed in order to obtain the marginal distributions of the random variables.

3.4.1.2 Deterministic security assessment

The flowchart of DSA algorithm for each MC simulation is presented in Figure 3.5. The methodology involves performing a detailed deterministic load flow (DLF) for each MC sample. Many DLF computations are performed to have a high level of accuracy, and is thus computationally expensive. The DSA algorithm consists of: i) full AC PF computations, ii) automatic generation control (AGC) for restoration of power balance, iii) a cascading mechanism, and iv) two risk identifying tools. These risk identifying tools are explained in the next section.

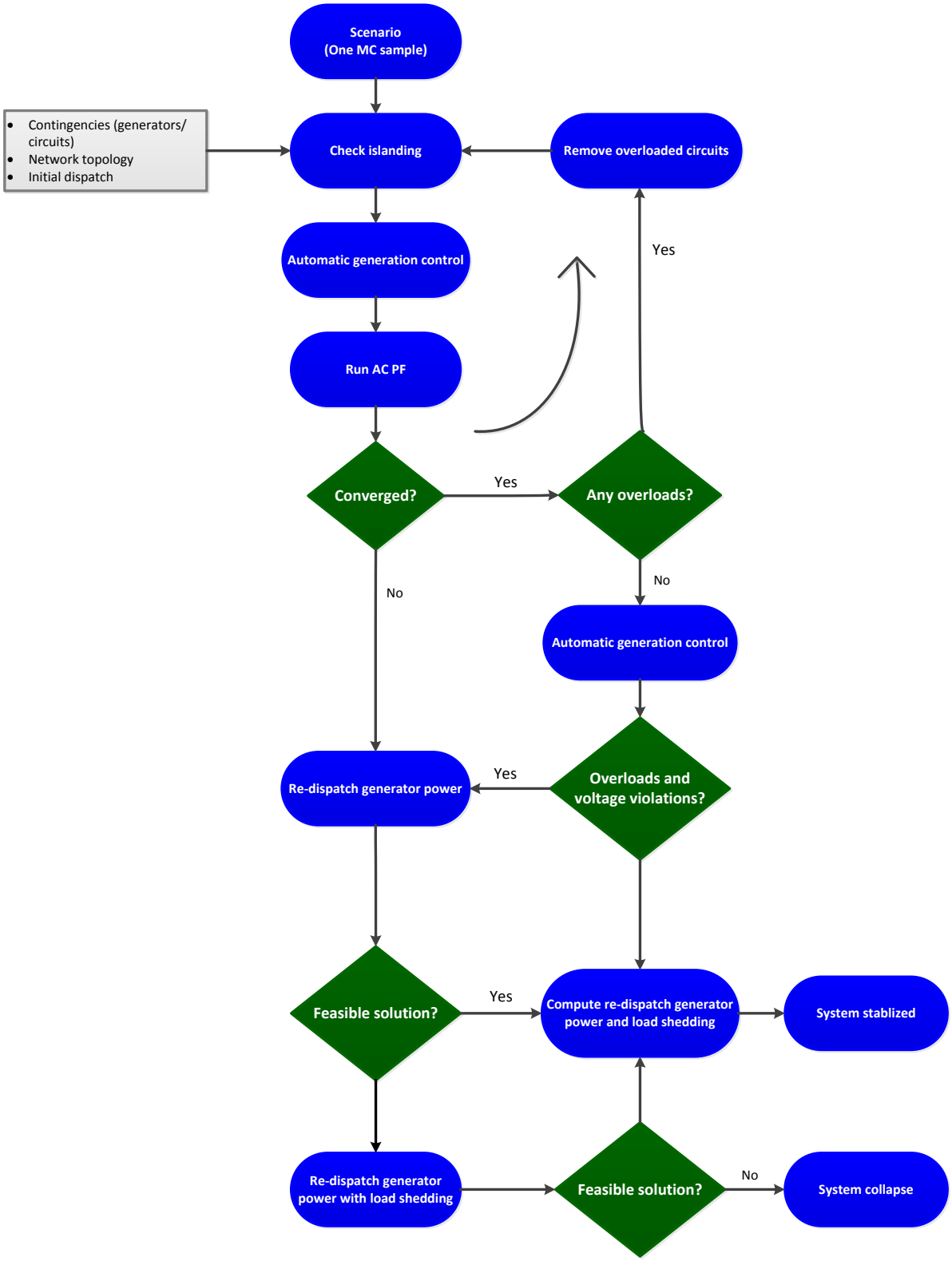

Figure 3.5: Flowchart of RBSA methodology for one MC sample.

3.5 Two risk identifying tools

The proposed RBSA methodology employs two risk identifying tools: i) Tool I: a fast-screening tool using the concept of severity functions, and ii) Tool II: a detailed analysis tool using extended AC OPF to provide valuable information to TSOs on expected curative measures. The details are as follows:

- Tool I uses McCalley's concept of severity functions [40]. These functions are employed to quantify the severity associated with the following: i) circuit overloads, and ii) voltage violations. These functions are defined such that they start measuring severity if:

  - the power flows exceeds the thermal rating by a factor 0.9, i.e., the power flows approach their thermal limits. It is calculated by:

    $$x = \frac{P_l}{P_{l,max}}, \tag{3.8}$$

    where x is load factor, P_l represents the actual power flowing through the transmission line l, and $P_{l,max}$ represents the thermal rating of the transmission line l.

  - the bus voltage is close to either maximum voltage (V_{max}), or close to minimum voltage (V_{min}), i.e., the bus voltage magnitudes approach their maximum, or minimum limits. It is calculated by:

    $$y = \frac{V_b - V_{b,nom}}{s_b}, \tag{3.9}$$

    where V_b represents the true voltage at the bus b, $V_{b,nom}$ represents the nominal voltage at the bus b, and s_b is the permissible range of the voltages.

  The tool can be used to compute the probability of cascading events as well as the probability of islanding.

- Tool II is based on Kirschen's concept of risk indicators. To access the risk levels, the tool distinguishes the curative remedial actions into four categories:

  (i) No remedial measures;

  (ii) Remedial active re-dispatch;

  (iii) Remedial active re-dispatch plus lost active load;

  (iv) System collapse, or blackout.

  These risk indicators are implemented within the AC OPF framework, and provide valuable information on how to access the expected system risk in day-ahead operation. The expected amount of remedial re-dispatch of generator's active power is calculated by:

  $$E[active\ re-dispatch] = \frac{1}{N}\sum_{i=1}^{N} AR_i,$$

  where

  $$AR_i = \frac{1}{N_{gen}}\sum_{j=1}^{N_{gen}} (P_j^{post} - P_j^{pre}), \tag{3.10}$$

  is the expected amount of active re-dispatch for a MC sample i. In Equation (3.10) P_j^{pre} and P_j^{post} represent the amount of generator's active power before and after re-dispatching, respectively, N represents the total number of MC samples, and N_{gen} the total number of generators. Moreover,

this corresponds to the MC samples with risk levels 2, and 3, and is implemented within the detailed analysis of Tool II. The expected amount of curative load shedding is calculated by:

$$E[Load\ shed] = \frac{1}{N} \sum_{i=1}^{N} LS_i,$$

where

$$LS_i = \frac{1}{N_{bus}} \sum_{k=1}^{N_{bus}} (P_k^{post} - P_k^{pre}), \tag{3.11}$$

represents the expected load shed for a MC sample i. In Equation (3.11) P_k^{pre} and P_k^{post} represent the amount of load's active power before and after load shedding, respectively, and N_{bus} the total number of buses. Moreover, this corresponds to the MC samples with risk levels 3, and is implemented within the detailed analysis of Tool II. For samples with risk levels 4, the lost active load for MC sample i is calculated by:

$$LS_i = \frac{1}{N_{bus}} \sum_{k=1}^{N_{bus}} P_k^{pre}.$$

Moreover, in this work it has been proposed to adapt the HVDC set-point as a part of curative (cost free) remedial action to avoid active re-dispatch and shedding of load.

Chapter 4

High-Voltage Direct Current (HVDC) technology

4.1 Overview

In this chapter, an overview of the HVDC technology, i.e., theory and modeling principles in order to understand the operation of the HVDC transmission using RBSA methodology is presented. The current practice concerning day-ahead HVDC grid operation used by TSOs in determining the HVDC set-points is discussed.

4.2 HVDC grid operation and power flow controllability

In contrast with the AC grids, the DC grids provide fast controllability of active and reactive power flow which in turn improves the operational security of the grid by preventing congestions and risky events such as cascading. Additionally, the HVDC technology provides ancillary services to the existing AC infrastructures, and helps in preventing the congestions on parallel HVAC transmission lines [47]. The HVDC technology supersedes the cost of expensive power electronic components such as converters and is expected to provide the best economical solution beyond the break-even distance of about 600-800 km for overhead transmission lines and about 50 km for submarine cables, as illustrated in Figure 4.1.

Valuable research has been conducted to study the complex interaction of HVAC-HVDC interlinked meshed power systems. In [48, 49], Beerten and fellow workers address the steady-state modeling of hybrid AC and DC grids, discuss the open source software package MatACDC that they developed, and it is emphasized that such tools are needed to be able to correctly analyze the steady-state interaction of complex interconnected hybrid systems. The proposed tool computes iteratively the interrelated AC/DC power flow solutions for multi-terminal HVDC (MTDC) systems embedded in existing AC networks. In [50], Roald and co-workers proposed a methodology for the corrective control of HVDC transmission lines and PSTs when subjected to both forecast uncertainty and contingencies. These corrective control measures are based on affine control policies, where the set-points are adapted in response to the forecast error. In this work, we are focused on the determining the best HVDC set-point using AC OPF when the system is subjected to unavoidable uncertainty of inputs inherent to day-ahead forecasting.

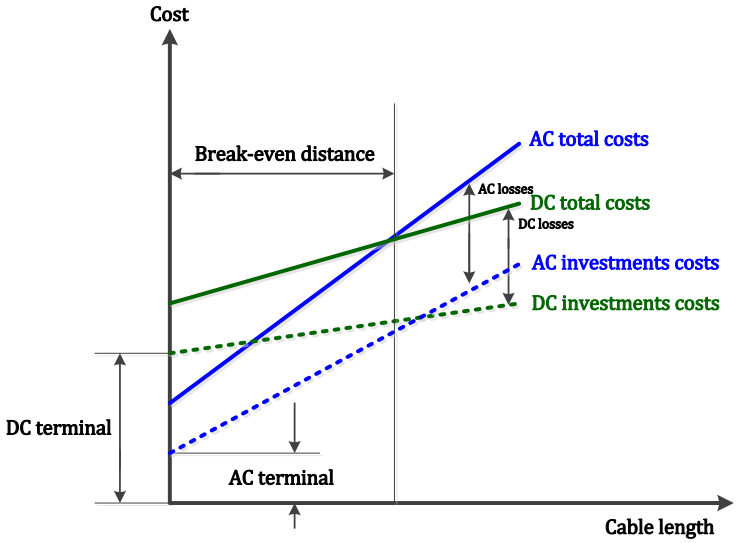

Figure 4.1: Cost comparison of HVAC and HVDC transmission technology.

Nowadays, the cooperation between the neighboring as well as non-neighboring TSOs is playing a vital role in the transmission planning of the HVDC interconnections in meshed hybrid power systems [51]. Usually, the HVDC interconnections are operated between two energy markets based on the contractual agreement or market regulations, and, depending on the operating region, the active power set-points are regulated either by one or more TSOs. Market regulations limit the inherent controllability of the HVDC technology to relieve the network from risky operating states during the occurrence of severe contingencies. In [52] a coordination methodology is proposed, and it is shown more international interaction among TSOs is needed for determining the optimal operating set-points for cross-border HVDC interconnections.

ENTSO-E published a document to serve as a guide for software developers to build an IT platform to exchange information relative to HVDC schedules between multiple TSOs. It identifies four main steps that TSOs should take into account when determining the HVDC schedules based on day-ahead operation: i) HVDC constraint determination, ii) Cross-border capacity computation, iii) HVDC configuration and iv) HVDC schedule calculation. Furthermore, it states that depending on TSOs the same steps could be carried out again for purposes of re-matching and re-generation in intraday operation [53].

Additionally, in Appendix 8 of the Nordic System Operation Agreement (SOA) [54], the trading capacity on the HVDC connections is limited to a maximum value of 600 MW per hour. This restriction in the trading capacity has been imposed to deal with the flexible controllability in HVDC line flow with respect to the AC networks, as this might introduce significant power deviations in HVDC power transfer. This could make it for TSOs more difficult to handle the balance regulation of the meshed interlinked systems. Therefore, ramping constraints of 600 MW per hour are imposed on the trading plans for the cross-border Nordic HVDC interconnections. For example, there is a system operation agreement for the SwePol HVDC connection installed between Sweden and Poland. This agreement contains the information on the system operation regulations such as technical operational limits, emergency control functions and capacity allocation. This HVDC connection is regulated biyearly by the respective TSO, and is isolated from the intraday capacity allocation. More details on the transmitted HVDC active power and the ramping rate are given in Article 9 of the network code on HVDC, published by ENTSO-E [55].

As can be understood, the current practice concerning HVDC operation does not allow TSOs to determine which HVDC set-point gives the highest security of the power system when it is subjected to the unavoidable uncertainty of inputs (fluctuations in load) inherent to day-ahead forecasting. For all operating conditions, the power flow schedules between the HVAC and HVDC power systems are based on the pre-defined converter set-points [56]. Moreover, the HVDC interconnections such as, EstLink 1, EstLink 2, SwePol and NordBalt are generally operated to its maximum NTC value to export power across cross-border, further restricting TSOs to adapt the HVDC set-points in response to the forecast uncertainty [57]. Therefore, the proposed RBSA methodology can be used in determining the overall "best" HVDC set-point and help the power system to achieve the highest security level under all possible uncertainties.

4.2.1 HVDC Topology: LCC vs. VSC

There are two main topologies for an HVDC transmission system:

- Line Commutated Convertor (LCC);
- Voltage Source Convertor (VSC).

LCC-HVDC is a mature technology with thyristor-based commutation [11]. It needs a strong AC grid with adequate short circuit capacity, and reactive power compensating components to avoid the risk of commutation failures. LCC-HVDC systems can allow the transmission of bulk power over long distances, and exhibits relatively low losses. The DC current is kept constant, while the polarity of DC voltage is altered to control the power flow. Moreover, it is inconvenient to operate a multi terminal LCC-HVDC system with continuous change in power flows. Figure 4.2 illustrates the LCC-HVDC converter topology.

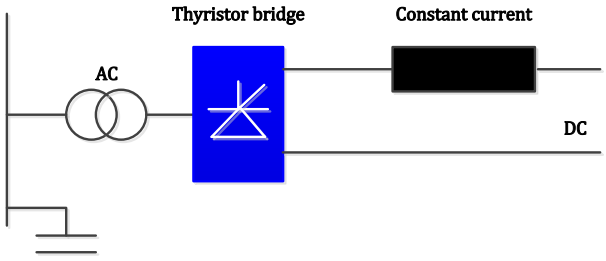

Figure 4.2: LCC-HVDC converter topology.

VSC-HVDC technology is based on fully controlled insulated-gate bipolar transistors (IGBTs) [11]. It uses high-frequency pulse width modulation (PWM) control and henceforth exhibits the flexibility in the power flow. This flexibility in the power flow of the converter stations makes this technology more suitable for a highly meshed interconnected electricity system. Moreover, it is also attractive from the market perspective considering that VSC-HVDC technology allows to control the active power flow faster than the LCC-HVDC technology. As active and reactive power can be controlled independently, this technology can exhibit the operations on weaker networks. Figure 4.3 illustrates the VSC-HVDC converter topology.

For these reasons, VSC-HVDC technology is preferred over LCC-HVDC and is most often used in new HVDC transmission systems [11]. In this work we also consider VSC-HVDC technology only.

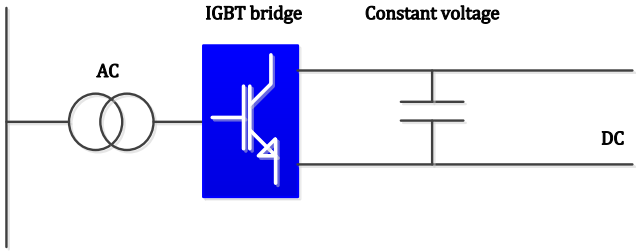

Figure 4.3: VSC-HVDC converter topology.

4.3 HVDC transmission line modeling concepts

4.3.1 Steady state VSC-HVDC transmission line model

A VSC-HVDC transmission line model consists of two voltage-source converter stations connected to the AC bus through a DC overhead line or cable. One converter in VSC-HVDC model operates as a rectifier, whereas the other converter operates as an inverter. They allow the transfer of constant DC power from rectifier to inverter station with high controllability. The VSC-HVDC converters are represented by complex AC voltage sources connected to the AC bus of the network through a transformer impedance. They are modeled as ordinary generators which extract or inject active and reactive power.

In VSC-HVDC converters, two independent control loops are employed for the regulation at the converter stations, namely the active and the reactive control power loop [58]. In the active power control loop, one converter controls the injected active power at the AC side of the grid whereas the other converter controls the magnitude of DC voltage. In the reactive power control loop, both the converters operate independently controlling either the injected reactive power or the voltage magnitude at the AC side of the grid. Combining the aforementioned, each converter has an ability to operate either as a PQ or PV node. As a PQ node, the converter is set to control the active and reactive power while as a PV node, the converter is set to control the active power and the magnitude of AC voltage. In either case, if one converter is set to control the active power flows, then the other will be set to regulate the DC voltage of the point-to-point HVDC system.

The PQ capability chart determines the operating area of VSC-HVDC transmission line by controlling the flow of the active and reactive power [59]. The maximum reactive power that either can be absorbed or injected is about 0.5 p.u. of the rated power of the VSC-HVDC light configuration [60]. The upper and lower bound for the voltages should be set within the specific boundary limits.

In this work, we also set the maximum and minimum of reactive power to 0.5 p.u. of the HVDC line rating. Furthermore, we set the converter voltage limits equal to 1 p.u. These limits were chosen in [61] as well.

4.3.2 VSC-HVDC transmission line model in MATPOWER

There are several ways to model a steady state VSC-HVDC transmission line in the load flow analysis. By leaving out details and assumptions for the converter data discussed in [62], the most precise model for the VSC-HVDC transmission line can be reduced to the easiest model, as shown in Figure 4.4. A simple mathematical representation of the VSC-HVDC connection has been used by MATPOWER [63]. This VSC-HVDC model provides us the desired accuracy in power flow simulations.

In MATPOWER, the steady-state VSC-HVDC transmission line is modeled as a pair of coupled generators (PV buses) with opposite sign of active power injection. One converter extracts active power from one end of the line, whereas the other converter injects active power to the other end of the line. Concerning the losses of the HVDC line: MATPOWER defines a linear relationship for the active power loss in the VSC-HVDC transmission line, as given in Eq. (4.1) and Eq. (4.2).

$$P_n = P_m - P_{loss}, \tag{4.1}$$

$$= (1 - l_1)P_m - l_0, \tag{4.2}$$

where P_m is the active power extracted from bus m and P_n is active power injected to bus n, and l_0 is constant loss coefficient and l_1 is linear loss coefficient.

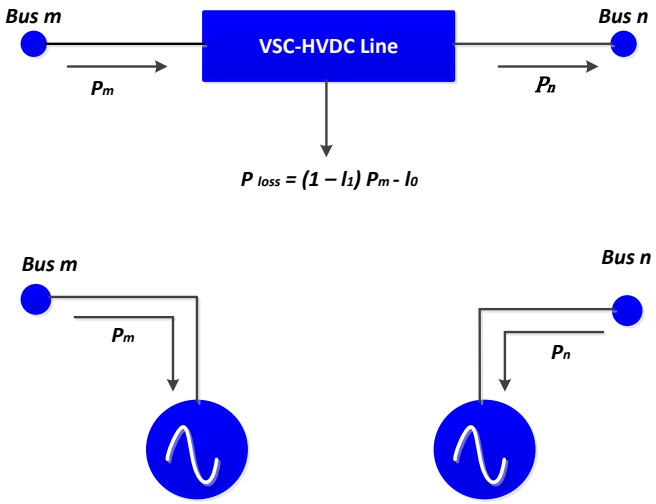

Figure 4.4: MATPOWER model of VSC-HVDC transmission line.

As the HVDC line is modeled as a pair of generators, the active power output can be controlled, as well as the voltage set-points. If, in the load flow equations, the constraints for reactive power output of any of the generators are reached, then the respective end of the VSC-HVDC transmission line operates as a PQ bus. Hence, both active and reactive power output of each of the two generators are controlled. Combining the aforementioned, the VSC HVDC transmission line can thus operate either in the PQ control mode or in the PV control mode. In the AC OPF problem formulation the inclusion of a VSC-HVDC transmission line is equivalent to the inclusion of a set of two ordinary generators in the network. Hence, the constraints taken into consideration for the HVDC line during AC OPF are the exact same as for ordinary generators:

(i) Constraints for maximum and minimum amount of active output;

(ii) Constraints for maximum and minimum amount of reactive output;

(iii) Voltage set-point of each of the two generators must lie within the same range as the bus they are connected to;

(iv) Voltage angle of each of the two generators must be within the same range as the bus they are connected to.

There are no additional costs for the VSC-HVDC dummy generators which are added to the objective function during AC OPF. These generators can attain any value (within bounds), which results in minimization of the objective function. This means that, for example, if the objective function is cost efficient dispatch (minimization of active power generation costs), then the other generators, the loads and the constraints on the elements determine how much power must be subtracted from the grid and injected into the grid by the two dummy generators so that the cost function attains lowest overall costs. Thus, the steady-state VSC-HVDC transmission line that has been modelled in MATPOWER [63] is employed in the proposed RBSA methodology to quantify system risk inherent to day ahead forecasting.

Chapter 5

Experiments and results

5.1 Overview

In this chapter, the proposed RBSA methodology based on Monte-Carlo sampling is employed to investigate the security of the system and to quantify the expected system risk in the operational day-ahead planning, taking into account load and RES forecast uncertainty and dependence of system in-feeds. Several case studies are performed to analyze how incorporation of HVDC transmission can be used as a smart grid solution to improve power system security and lower the risk in different adjacent areas. Moreover, the results obtained from the study reflect the need to properly adapt the HVDC set-points in response to the actual operating situation, as it can be quite different from the day-ahead point forecast as a result of uncertainty in load and RES in-feeds.

5.2 Experimental setup

In this section the setup of the experiment is analyzed. We first describe the implementation and hardware used for the experiment, followed by a description of the test system and its adjustments, and finally we present the experimental results of our analysis.

5.2.1 Implementation and hardware

The RBSA methodology has been modeled in MATLAB using the MATPOWER toolbox [63]. The numerical experiments are performed on a desktop computer of a quad-core 3.50 Ghz Intel(R) Core(TM) i5-4690 processor and 8 GB RAM.

5.2.2 Test system and its adjustments

For the case studies, the IEEE 24-bus reliability test system is used, see Figure 5.1. This system comprises 24 buses, 38 circuits (transmission lines and transformers), 32 thermal generators and one synchronous condenser. The system is divided into two zones: Zone 1 and Zone 2. More details on the test system can be found in the Appendix A. A single replacement of HVAC line 23-12 (right part of system) by the HVDC transmission line is considered in order to facilitate more transfer of active power from zone 2 to zone 1. This line seems to be the best candidate of the 24-bus system to be replaced as: i) it has a

decent capacity (500 MW), ii) it has one of the longest line lengths (100 km) in the entire system, iii) there is a big generation plant connected to it at what is in the base case the “sending end”, and iv) it is an important line to transport energy from Zone 1 to Zone 2 and vice versa; it is directly connected to the tie-station.

The following scenario is considered:

- The load in Zone I is increased by 20%, and the load in Zone II is decreased by 20%;
- The generation in Zone I is decreased by 20%, and the generation in Zone II is increased by 20% of the original capacity;
- The generation cost in Zone I is increased by 20%.

Because of the high demand in Zone I, higher generation costs, and less generation capacity within this zone, a scenario is created in which significant power flows are observed cross-border, i.e., the HVDC transmission line will inject “cheap” power from Zone 2 into Zone 1, where generation is more expensive.

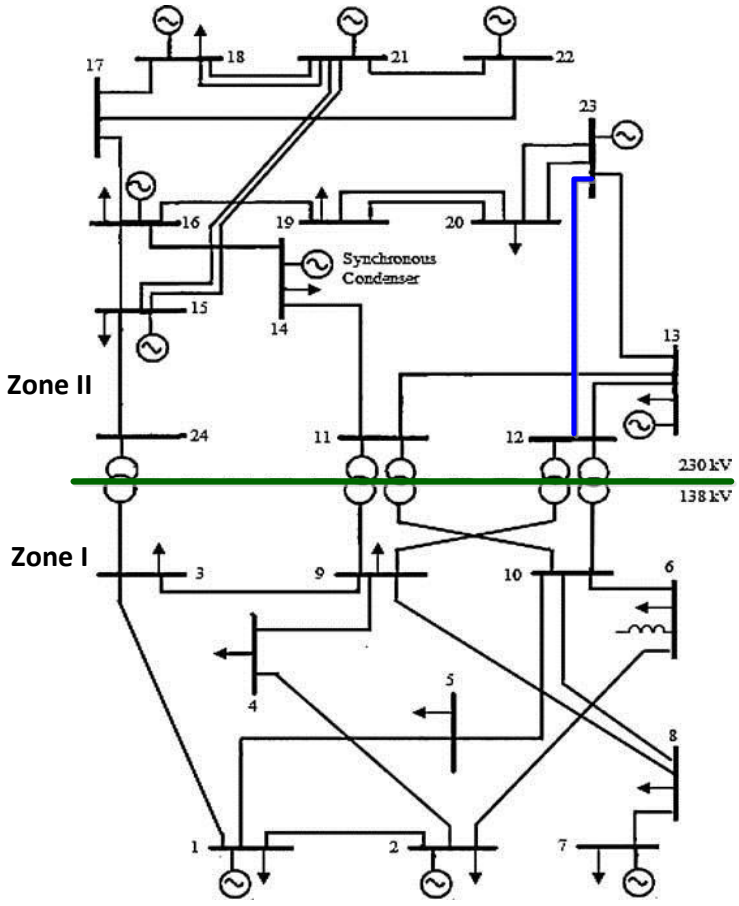

Figure 5.1: The two-zone IEEE 24-bus reliability test system with HVDC line between buses 23 and 12 (blue).

5.2.3 Result visualization

There are several graphical display functions included in the proposed RBSA methodology to provide valuable information to TSOs on how to steer the system into a risk-averse state. The graphical interpretation of the results are visualized using:

- GUI color risk-snapshots of the system displaying the regions of highest system stress on a nodal level;
- Iso-risk plots displaying the risk for 2D study parameter studies;
- Empirical distribution functions of quantities of interest, e.g., line loading, bus voltage magnitude, curative re-dispatch of active generation for each simulated grid point.

Moreover, for each simulated grid point, the results can be visualized in a transparent manner by giving a detailed analysis using the following criteria:

- Overloaded circuits/branches (transformers and transmission lines) per zone;
- Participating generators in curative re-dispatch;
- Load curtailment.

5.3 Case studies

In this section the following three case studies are investigated:

(i) Sensitivity analysis on HVDC set-points;

(ii) Adjustment of HVDC set-points by TSOs as part of curative remedial actions;

(iii) A 2D study with two HVDC transmission lines.

It is shown how the proposed RBSA methodology can be used in determining the best HVDC set-point when it is subjected to the unavoidable uncertainty of inputs (fluctuations in infeeds) inherent to day-ahead forecasting. For all the case studies, we first compute a cost efficient dispatch assuming a central dispatch market which is planning the system based on the expected average load at the buses, i.e., point forecasts. Moreover, the default AC PF solver is replaced by a custom load flow solver based on MATLAB's fsolve() routine, and MATPOWER's default AC OPF is replaced by the interior point solver IPOPT from the COIN library [64]. The flowchart of the proposed HVDC-RBSA methodology is presented in Figure 5.2.

5.3.1 Case study 1: Sensitivity analysis on HVDC set-points

In this case study we perform sensitivity analysis on HVDC set-points by investigating:

(i) **Comparison of "security versus markets dilemma"**: which set-point is the best compromise between cost and risk;

(ii) **Impact of forecast uncertainty and correlation**: which set-point performs the best in different scenarios (combination of HVDC set-points and, forecast uncertainty and correlation).

It must be noted that HVDC set-point must remain fixed during execution of the RBSA algorithm; in this first study the set-point is not considered to be adaptable by TSOs.

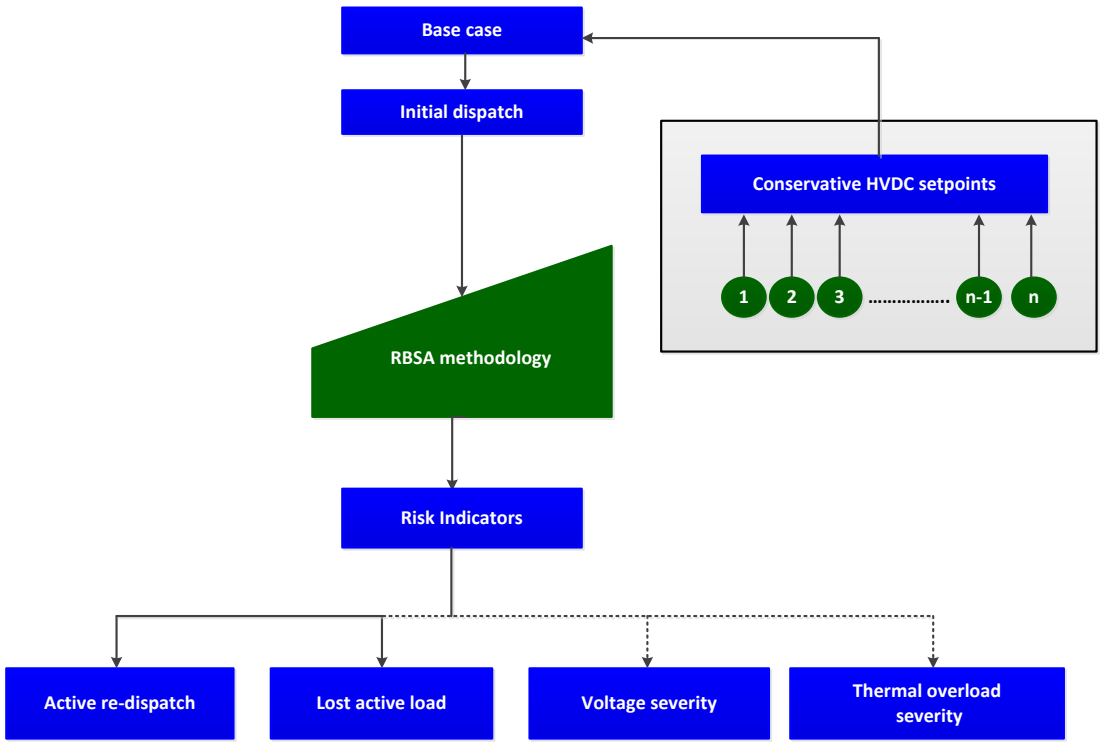

Figure 5.2: Flowchart of proposed HVDC-RBSA methodology.[1]

5.3.1.1 Part 1: Comparison of "security versus markets dilemma"

In this part of the case study we investigate how incorporation of HVDC transmission can affect the overall system risk, or risk in different areas/zones. We perform a Monte-Carlo simulation with the proposed RBSA tool to assess the HVDC set-points in day-ahead operation. Here, we use the IEEE 24 bus reliability test system with the same adjustments as described in Section 5.2.2.

5.3.1.2 DSA setup

The key features of the DSA algorithm at the core of the RBSA tool are:

- Active re-dispatch is implemented within an extended AC OPF formulation with a cost penalty term of 1 per MW;
- Lost active load is implemented within an extended AC OPF formulation with a cost penalty term (the highest penalty) of 1000 per MW.

It must be noted that the cost penalty terms should be set to sufficiently large values. Arbitrary numbers can be set by the operators, depending on the costs of the curative remedial actions. Here, the lost active load has the highest penalty as we assumed that TSOs would use this alternative as a last resort to avoid the risky system states.

5.3.1.3 Stochastic setup

Operational uncertainty is introduced to the system by considering uncertainty of in-feeds. For the numerical experiments, the snapshot data, i.e., point forecasts are assumed to be normally distributed.

[1] It must be noted that in this thesis, the analysis is focused on two risk indicators: i) active re-dispatch, and ii) lost active load. However, the proposed HVDC- RBSA methodology can be used to determine thermal overload severity, and voltage severity as well.

The point forecast at every bus $m = 1, ..., n_b$ is replaced by a normal marginals to indicate the uncertainty in the base case, given by:

$$P_m \sim N(\mu_m, \sigma_m), \qquad \sigma = f \,.\, \mu_m \tag{5.1}$$

where P_m is the active load at bus m, μ_m is mean of the active load, and σ_m is the magnitude of the standard deviation, i.e., $f = 0.15$ (15% of mean). Furthermore, we consider a zone-wise correlation matrix with rank correlation $\rho = 0.70$, i.e., all buses within the same zone are equally dependent on each other, as discussed in Section 3.4.1.1.

5.3.1.4 Case setup

Given the point forecast (the "best guess") of the operational situation tomorrow, two scenarios are investigated:

(i) **"Market optimal"**: The HVDC set-point is computed at the same time with the dispatch of active generation using AC OPF with an economic objective function;

(ii) **"Security optimal"**: A fixed HVDC set-point is considered, and selected prior to computation of the power dispatch. By doing so, a sensitivity analysis is obtained which can be used to determine those HVDC power set-points that come with the lowest risk. It must be noted that as the OPF is forced into a certain direction, probably the OPF cannot attain its economic best solution; it will attain a sub-optimal dispatch, however, this may result in higher security of the system.

A 1D grid consisting of 25 grid points is obtained by varying the HVDC set-point in appropriate (small) steps, i.e., 25 MW. For every grid point we generate a PLF consisting of 5.000 MC samples *(P,Q)*.

5.3.1.5 Results and reflection

For the following evaluation, we perform 25 MC simulations (25 grid points) in order to determine the system risk associated with every HVDC set-point. For every grid point we ran a MC simulation with 5.000 samples. Essentially, by doing so, for every HVDC set-point we obtain two values: i) risk (in terms of expected active re-dispatch, and lost active load) and ii) generation dispatch costs. This allows for a detailed comparison "risk vs. costs" using a 1D plot, as presented in Figure 5.3. It is seen that the expected amount of active remedial re-dispatch gradually increases from point A to point B, and the generation dispatch costs gradually decreases from point C to point D, see Figure 5.3 (left). A similar trend can be identified for the expected amount of curative lost active load, see Figure 5.3 (right). Thus, much higher risk is observed for the most optimal "cost set-point", while lower risk is observed for the most optimal "security set-point". In Table 5.1 a comparison for the "security optimal" and "market optimal" is presented[2].

Table 5.1: Comparison of "security optimal" and "market optimal" HVDC power set-points.

	Grid point	Generation dispatch cost[$/hr]	Active re-dispatch [MW]	Lost active load [MW]
Security optimal set-point	18	59596	26.89	1.78
Market optimal set-point	25	59332	39.77	2.45

[2] As it can be seen from Table 5.1, for our simulations, there is a slight difference in the generation dispatch costs. However, in this thesis, it is emphasized, that there is a need for a security check to evaluate the market results.

The results obtained from the comprehensive analysis tool for: i) grid point 18, i.e., the optimal "security set-point", and ii) grid point 25, i.e., the optimal "market set-point" are shown in the following figures/tables:

- The zone-wise active re-dispatch and lost active load are presented in Table 5.2. It can be observed that the generators in Zone 2 contribute more in re-dispatching the active power in order to alleviate the problems associated with voltage violations in Zone 1. In addition, significant load is shed in Zone 1 to attain lower system risk;
- The average re-dispatch of active power per generator for the grid point 18 is estimated around 26.88 MW, see Figure 5.4 (left), where the red marker G1 and G2 represents the generators connected to bus 13, and bus 22, respectively. The average re-dispatch of power per generator for the grid point 25 is around 39.76 MW, see Figure 5.4 (right), where the red marker G3 and G4 represent the generators connected to bus 13, and bus 22, respectively. It must be noted that: at bus 13 and bus 22, the maximum generation is re-dispatched, and therefore these generators are particularly important to restore the systems security;
- The average lost active load at every bus for market-optimal set-point is estimated around 1.77 MW, see Figure 5.5 (left), whereas for security optimal set-point is around 2.45 MW, see Figure 5.5 (right). It must be noted that: the red marker L1 and L2 represent the bus number (bus 6) where the maximum load is shed to help the system to go to secure states;
- Figure 5.6 presents the number of overloaded circuits and Figure 5.7 presents the number of voltage violations for every bus of the test system. As it can be seen from the figures, thermal violations occur more often for the security optimal set-point than voltage violations. This means, voltage violations have a significant contribution to the overall system risk, which could be neglected if the risk assessment tools would have relied on DC approximations. The proposed RBSA methodology successfully traced the problems related to voltage violations at the buses. As bus 3 turned out to be the weakest bus, the comprehensive analysis of voltage magnitudes after and prior to RBSA check is illustrated in Fig 5.8. It must be noted that circuit 10, i.e., the line connecting bus 6 and bus 10 is one of the most critical branch in the entire network, which was also highlighted by the RBSA check;
- Figure 5.9 presents the probabilities for the causes of problem, i.e., overloaded circuits, voltage violations and non-convergence of power flows. In Figure 5.10 the probabilities of risk levels are illustrated. These figures provide a great insight of where the risk comes from. The red marker highlights the market optimal and security optimal set-points.

Table 5.2: Zone-wise re-dispatched active generation and lost active load.

Grid point	**Active re-dispatch [MW]**		**Load active load [MW]**	
	Zone 1	**Zone 2**	**Zone 1**	**Zone 2**
18	0.43	26.46	1.69	0.08
25	0.48	39.29	2.38	0.068

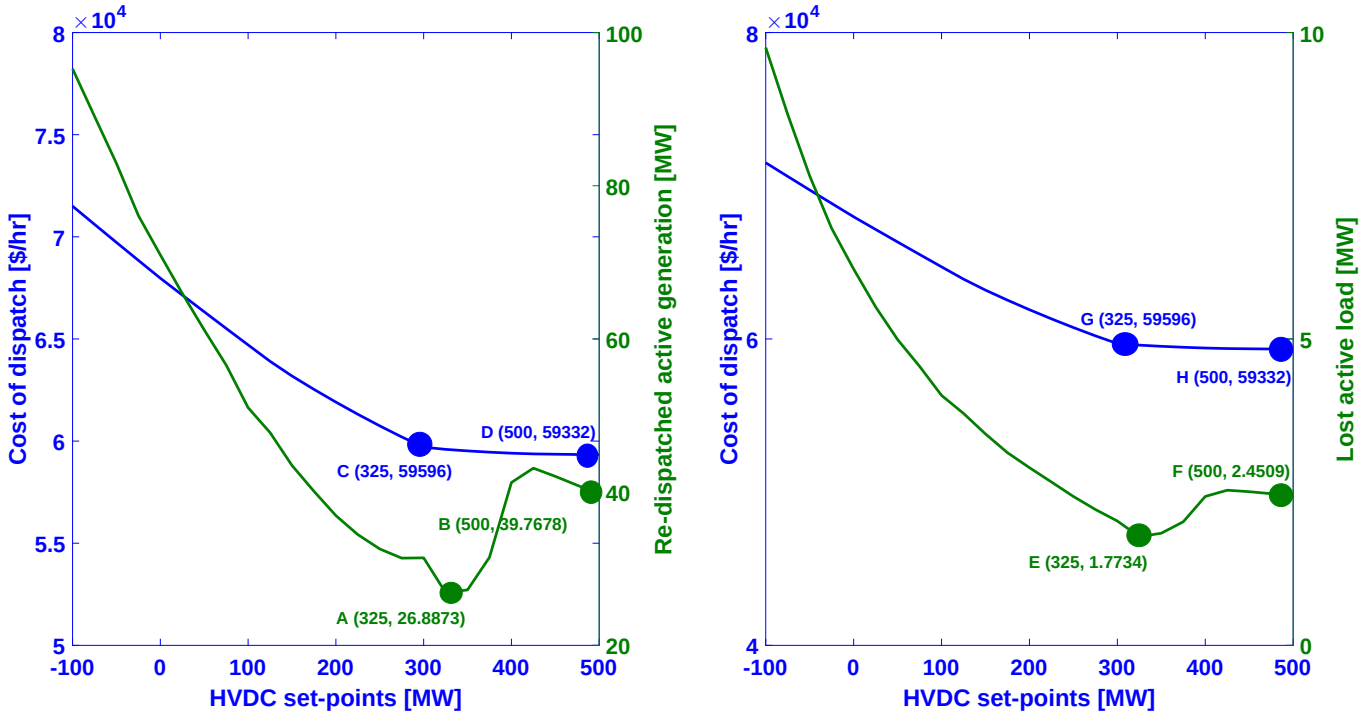

Figure 5.3: Comparison of dispatch costs and risk (active re-dispatch and lost active load).

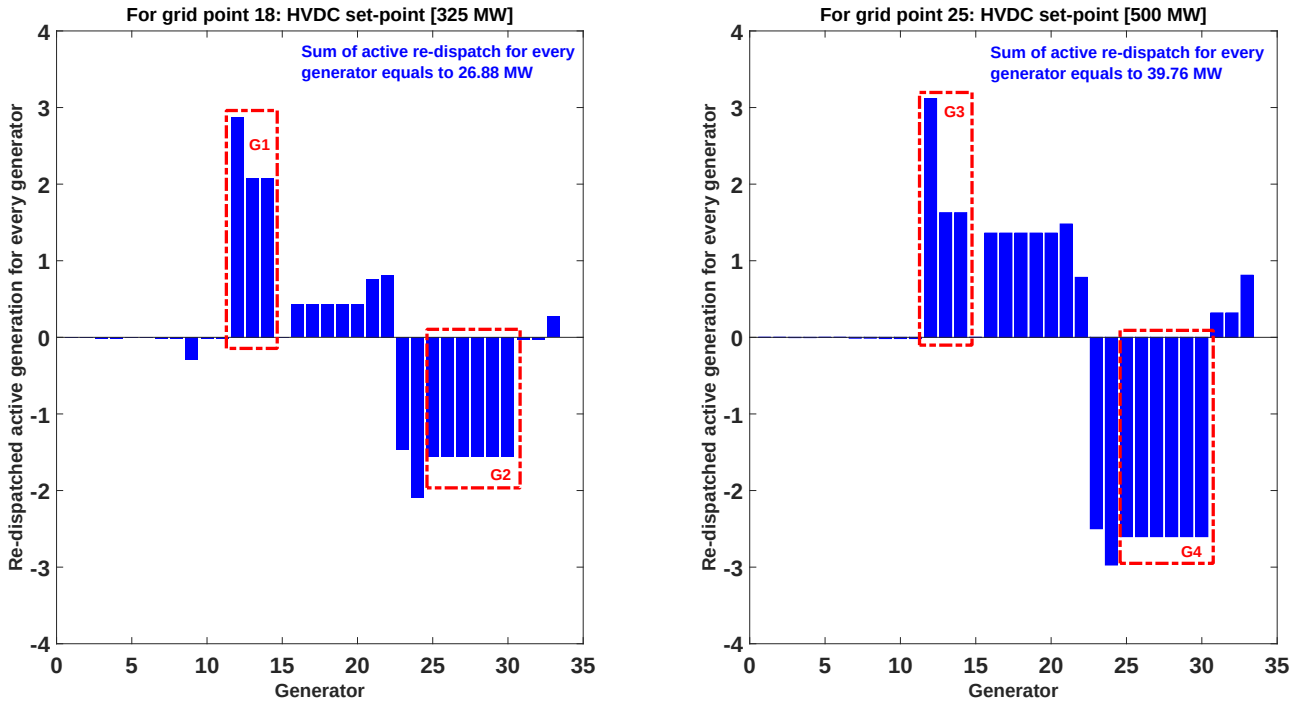

Figure 5.4: Re-dispatched active power for every generator.

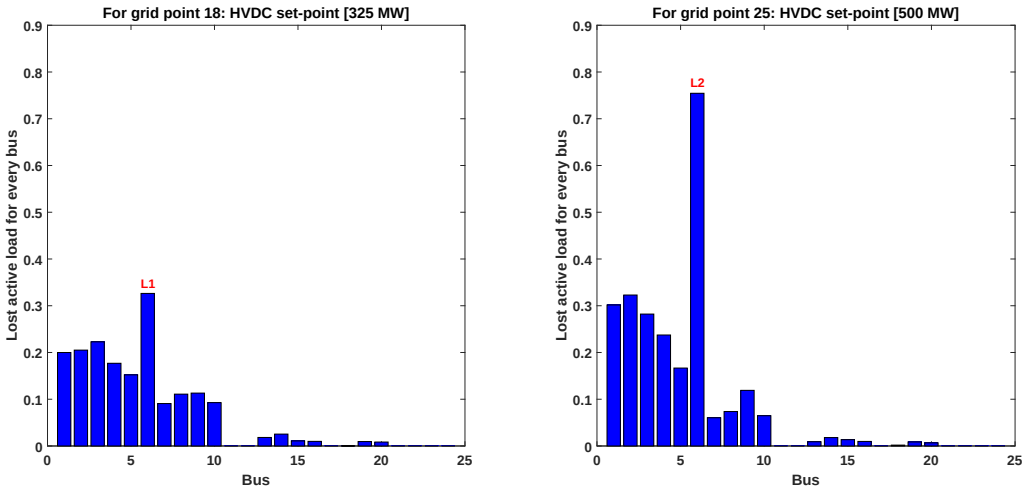

Figure 5.5: Lost active load for every bus.

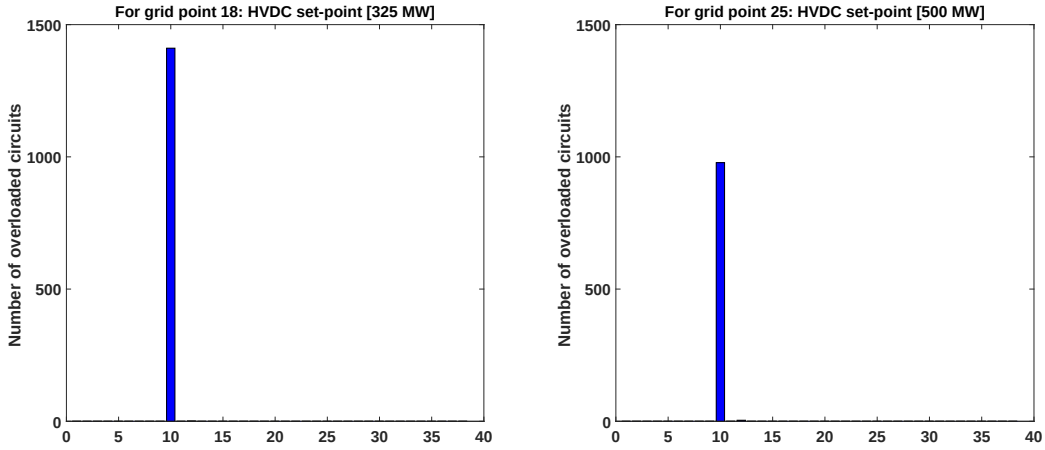

Figure 5.6: Number of overloaded circuits at every bus. Total number of MC-samples is 5000.

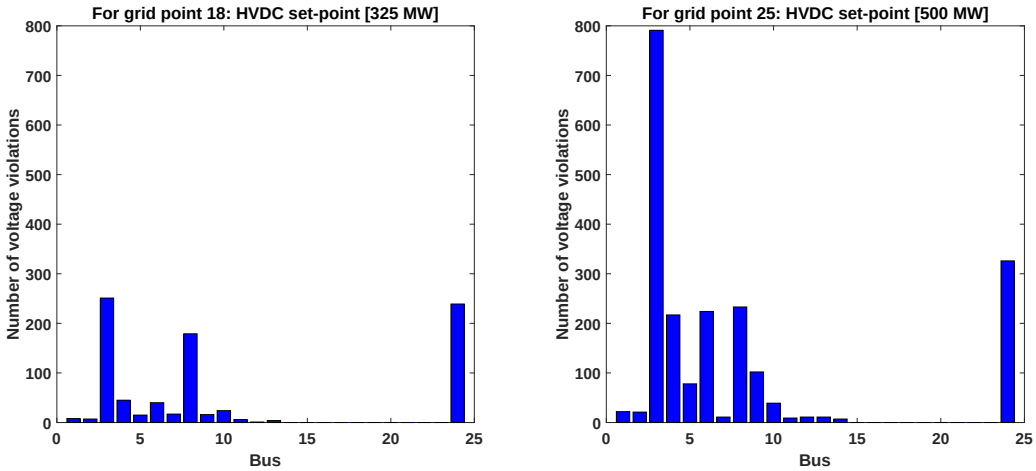

Figure 5.7: Number of voltage violations at every bus. Total number of MC-samples is 5000.

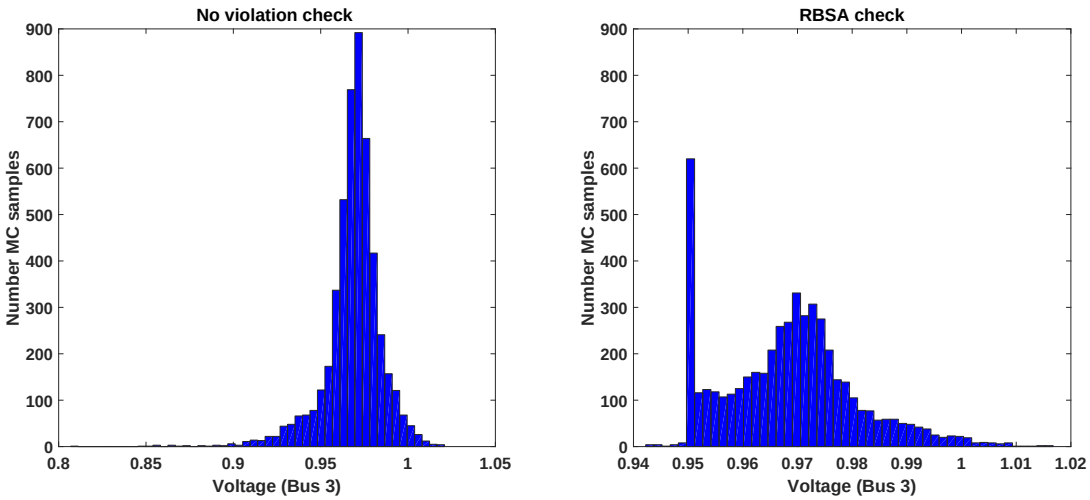

Figure 5.8: Improved voltage profiles at bus 3 with RBSA check.

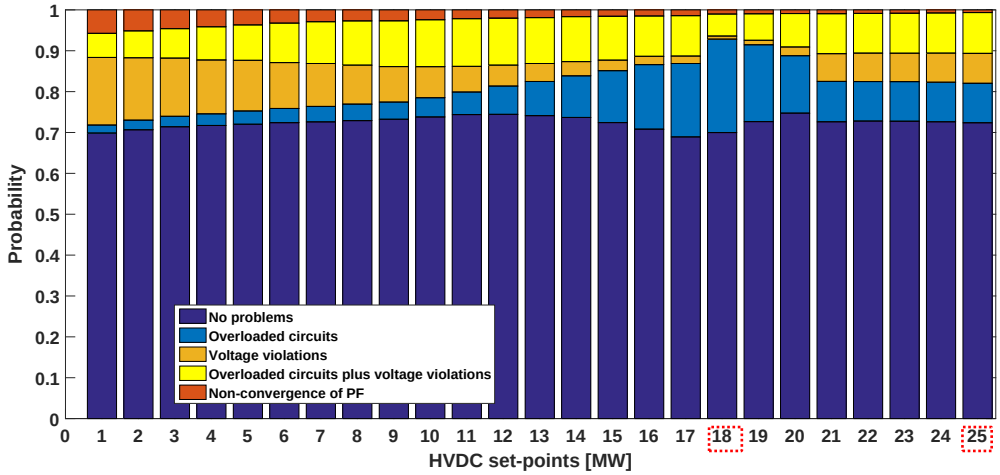

Figure 5.9: Probabilities for causes of problems in the system.

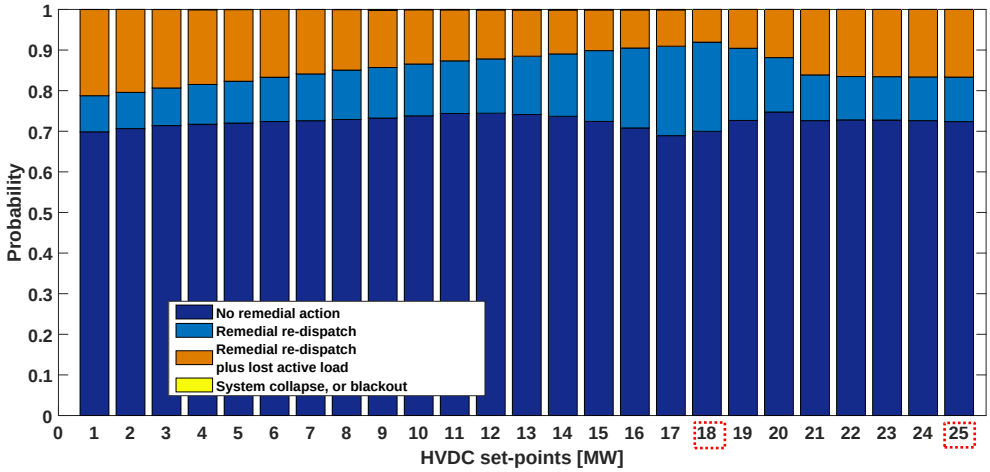

Figure 5.10: Probabilities of risk levels.

In order to provide more insight, we take the ratio of generation dispatch costs and risk to find the most “optimal HVDC set-point” on overall, i.e., the best compromise between cost and risk. As shown in Figure 5.11, the most “optimum set-point” that balances both cost and security is when the HVDC set-point is set to 325 MW. Ratio of cost and risk may help TSOs to identify / determine the "optimal set-point". By applying these set-points the operating point of the system moves to the one which comes with lowest risk, and lowest cost on overall.

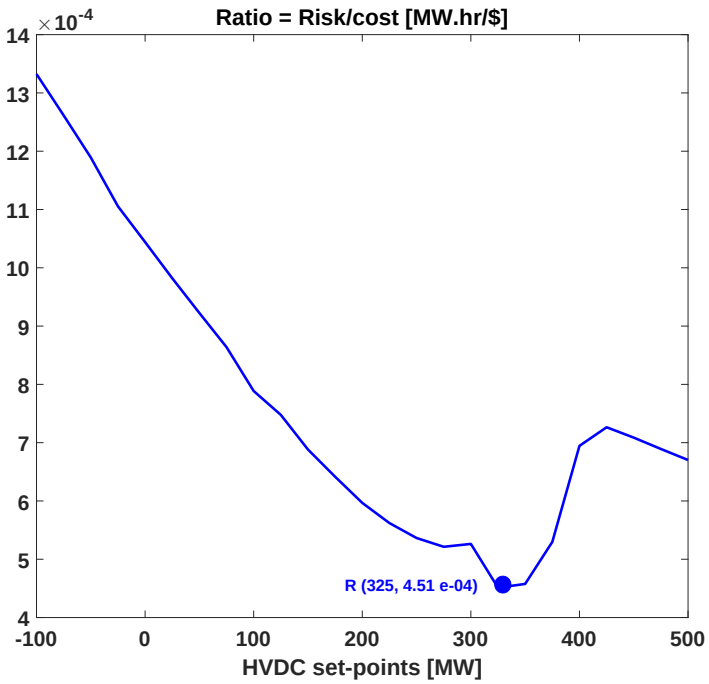

Figure 5.11: The best compromise between cost and risk is indicated by the blue dot.

5.3.1.6 Part 2: Impact of forecast uncertainty and correlation

In this part of the case study we assess the impact of forecast uncertainty and correlation on the expected system risk in day-ahead operational planning. Here, we use the same test system with the same adjustments, and the same DSA setup as described in part 1 of Case Study 1.

5.3.1.7 Case setup 1: Impact of forecast uncertainty

A 2D grid consisting of 25 × 11 grid points is obtained as follows:

- X axis: HVDC set-point is varied in appropriate (small) steps, i.e., 25 MW;
- Y axis: Forecast uncertainty is varied in appropriate steps, i.e., 0.02.

5.3.1.8 Results and reflection

For the following evaluation, we perform 25 × 11 = 275 MC simulations in order to determine the sensitivity of the expected system risk with respect to HVDC set-points and forecast uncertainty. For each grid a MC simulation is performed with 5.000 samples. Figure 5.12 presents the expected amount of remedial re-dispatch (see left) and the expected amount of curative lost active load (see right). It can be seen that when forecast uncertainty is high, the risk perhaps becomes higher. Moreover, the HVDC

set-points between 325 MW and 400 MW performs the best when the correlation is fixed to a value of 0.7.

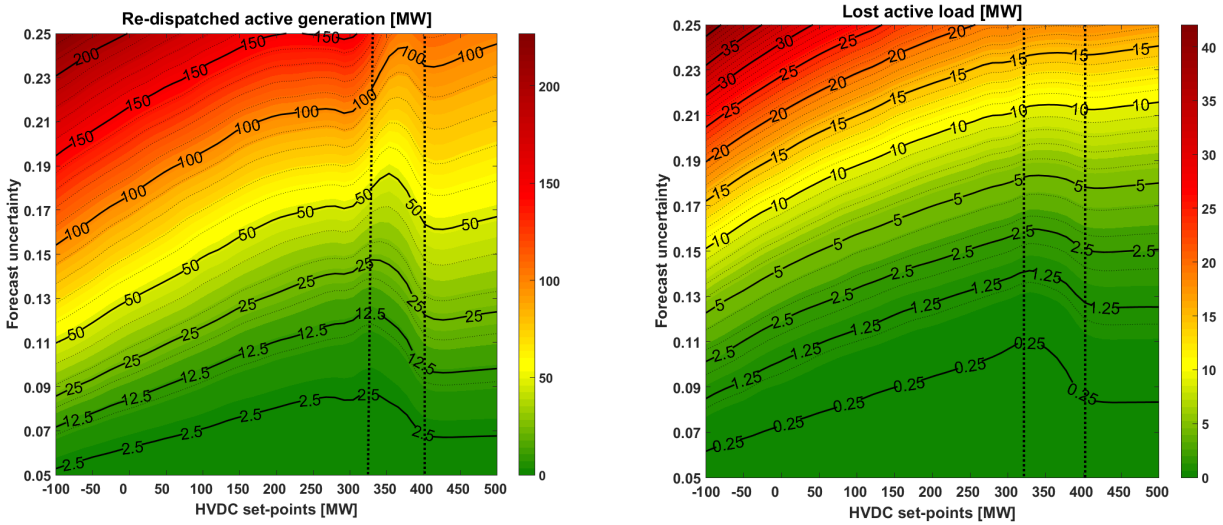

Figure 5.12: Impact of forecast uncertainty: Risk in terms of re-dispatch active load and lost active load.

5.3.1.9 Case setup 2: Impact of correlation

A 2D grid consisting of 25 × 11 grid points is obtained as follows:

- X axis: HVDC set-point is varied in appropriate (small) steps, i.e., 25 MW;
- Y axis: Correlation is varied in appropriate steps, i.e., 0.1.

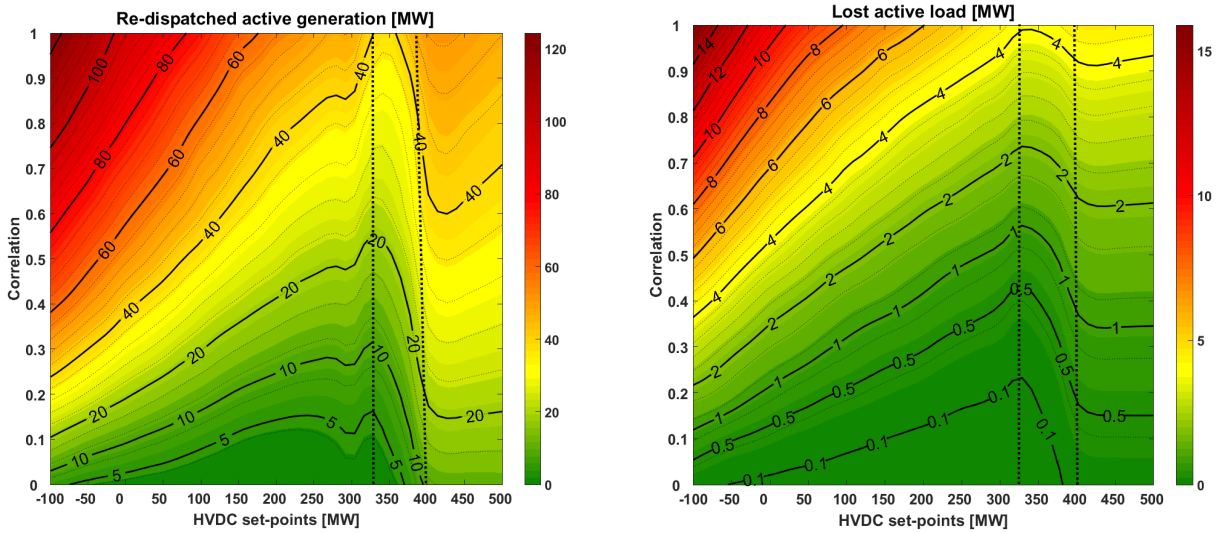

Figure 5.13: Impact of correlation: Risk in terms of re-dispatch active load and lost active load.

5.3.1.10 Results and reflection

In Figure 5.13, a similar trend for remedial expected active re-dispatch and curative lost load as described in Section 5.3.1.8 is observed with respect to the combination of HVDC set-points and correlation. It can be seen that the HVDC set-points ranging between 325 MW and 400 MW performs the best when forecast uncertainty is set to a value of 0.15. Thus, the market optimal set-point where HVDC link is operating to its full capacity does not necessarily provide the most secure set-point to steer the system away from risky situations.

5.3.1.11 Visualization tool

The visualization tool has been developed to display the regions of highest system stress on a nodal level. Figure 5.14 and Figure 5.15 present the GUI color average operating state for HVDC set-point 325 MW (= security optimal set-point) and HVDC set-point 500 MW (= market optimal set-point), respectively. For security optimal set-point, the re-dispatching of the generators, and the load shedding at the buses are highlighted using the color code, where the color brown corresponds to the generators and loads where the re-dispatching, and load shedding is maximum, respectively. It can easily be observed that bus 13 and 22 contribute maximum to re-dispatch, and maximum load is shed at bus 6, see Figure 5.14 (left). The load factor is shown in Figure 5.14 (right), where the lines 6-10, 16-17, and 16-19 have the highest load factor (green corresponds to the lowest, and red corresponds to the highest values for load factor). A similar trend can be observed for the market optimal set-point, where bus 13, 15, and 22 contribute maximum to re-dispatch, and again maximum load is shed at bus 6, see Figure 5.15 (left). Moreover, the critical lines remain almost the same as the security optimal set-point. A detailed analysis on the outcome of the generation dispatches, loads, voltage magnitudes at the buses, and power flowing through the lines are provided in Appendix B. Thus, by doing a sensitivity analysis for HVDC set-points; it can be concluded that TSOs would set the HVDC set-point to 325 MW as being the best compromise for both cost and security, and also with respect to the forecast uncertainty and correlation.

5.3.2 Case study 2: Adaptability of HVDC set-point by TSO as curative remedial action

In this case study we investigate how the adaptability of the HVDC set-points can enable TSOs to improve the system security under possible set of uncertainties. We perform a Monte-Carlo simulation with the proposed RBSA tool to assess the adaptability of HVDC set-point as a curative remedial action in day-ahead operation. Here, we use the same test system with the same adjustments, and the same stochastic and case setup as described in Case Study 1. Moreover, a level of risk is added to the four levels defined previously. We now have:

(i) No remedial measures;

(ii) Remedial HVDC adaptation;

(iii) Remedial re-dispatch;

(iv) Remedial re-dispatch plus lost active load;

(v) System collapse, or blackout.

It must be noted that the HVDC adaptation is inserted as the new level 2, so adapting the HVDC set-point is first tried, prior to curative remedial actions such as active re-dispatch and load shedding.

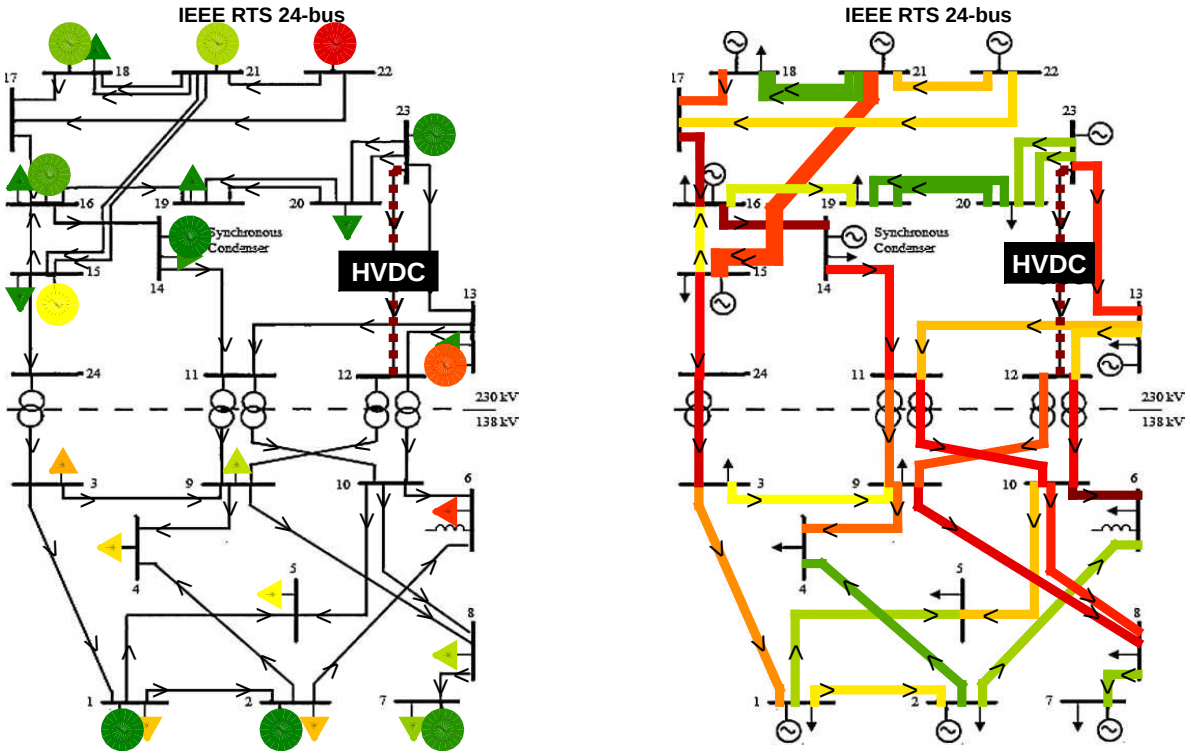

Figure 5.14: Average operating state when HVDC set-point is set to 325 MW.

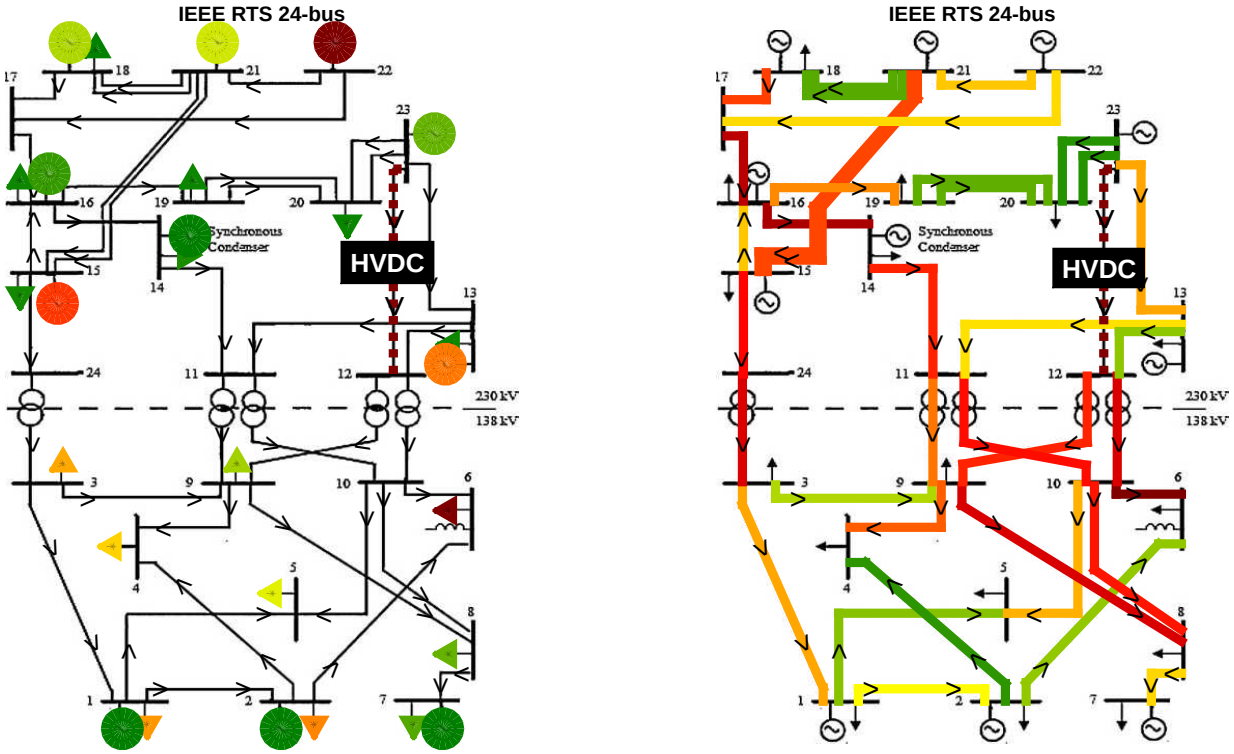

Figure 5.15: Average operating state when HVDC set-point is set to 500 MW.

5.3.2.1 DSA setup

The key features of the DSA algorithm consists of:

- HVDC set-point adaptation is enforced within an extended AC OPF formulation with a cost penalty term of 0 per MW. This corresponds to the MC samples with risk levels 2, implemented within the detailed analysis of Tool II;
- Active re-dispatch is implemented within an extended AC OPF formulation with a cost penalty term of 1 per MW. This corresponds to the MC samples with risk levels 3, and 4, implemented within the detailed analysis of Tool II;
- Load active load is implemented within an extended AC OPF formulation with a cost penalty term of 1000 per MW. This corresponds to the MC samples with risk levels 4 and 5, implemented within the detailed analysis of Tool II.

5.3.2.2 Result and reflection

For the following evaluation, we perform 25 MC simulations (25 grid points) to quantify system risk in the day-ahead security assessment when:

(i) The HVDC set-point is not able to adapt in curative remedial action, i.e., the "**dumb**" approach;

(ii) The HVDC set-point is able to adapt in curative remedial action, i.e., the "**smart**" approach.

In both the scenarios, for each grid point a MC simulation is performed with 5.000 samples. Essentially by doing so, we obtain a set of HVDC set-points in case HVDC adaptation (= "smart" approach) to resolve the problems. This allows for a detailed comparison between "dumb" and "smart" approach, see Figure 5.16 (green represents the "dumb" approach, and blue represents the "smart" approach). It is seen that the expected amount of remedial active re-dispatch is less for "smart" approach as compared to the "dumb" approach. Figure 5.17 presents the empirical PDF using 5.000 samples for HVDC set-point 325 MW (= security optimal set-point) where the big spike indicates that most of the time, there is no need for HVDC set-point to adapt; however, in few cases the HVDC power set-point must be lowered and occasionally, the full capacity of the HVDC link must be used to steer away from risky situations. By being able to adapt the HVDC set-point, we show that more serious and more costly remedial actions can be avoided (such as active re-dispatch, shedding of load). Therefore, the HVDC set-point should not be fixed to only a single value, rather it should be able to adapt to help the system go to secure states in response to all possible uncertainties in real-time situation.

5.3.3 Case study 3: 2D study with two HVDC transmission lines

The two-zone IEEE 24-bus reliability test system with HVDC line between buses 23 and 12 is stressed on right part of the system, as shown in Figure 5.14 and Figure 5.15. In order to reduce stress on one side of the system, another HVDC replacement on the left part of the system between buses 15 and 24 is considered. In this case study we investigate how the set-points of two HVDC transmission lines can work together to find the most optimum risk vs. cost operating set-points. We perform a Monte-Carlo simulation with the proposed RBSA tool to check how two HVDC set-points coordinate to steer the system away from risk. Here, we use the test system and the same DSA and stochastic set-up as described in Case Study 1.

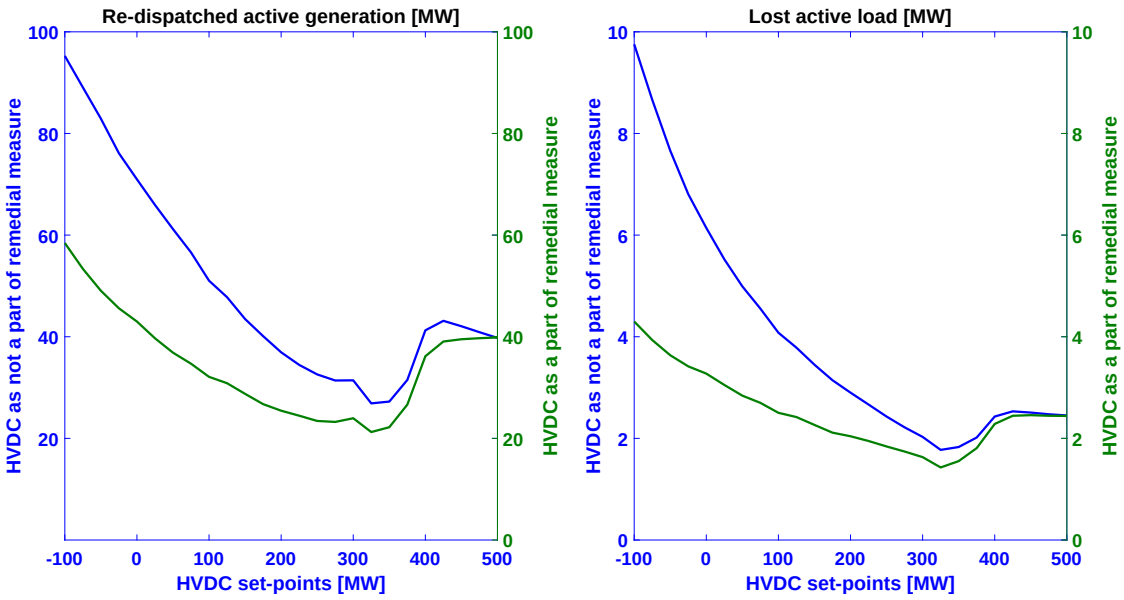

Figure 5.16: Comparison of "dumb" (blue) and "smart" approach (green).

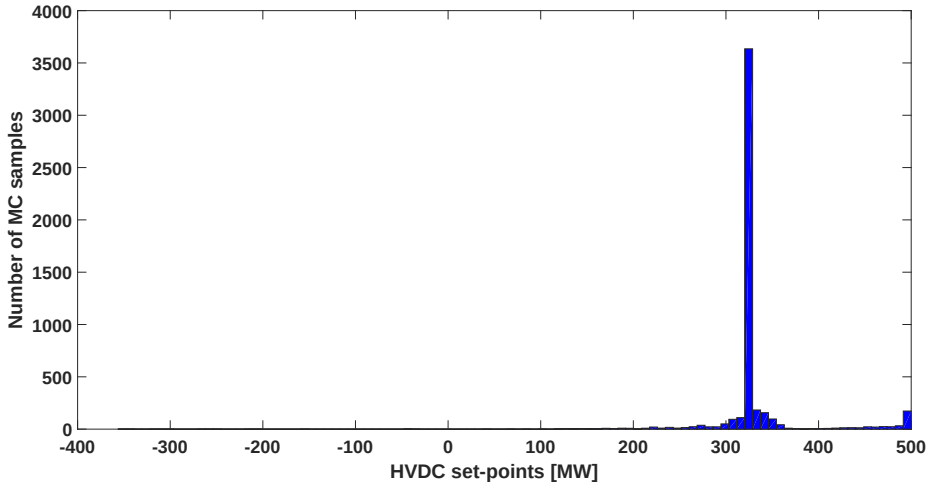

Figure 5.17: Adaptability of HVDC set-point 325 MW.

5.3.3.1 Case setup

A 2D grid consisting of 25 × 8 grid points is obtained as follows:

- Line 1 (Bus 23 to bus 12): HVDC set-point [-100, 500] is incremented in steps of 25 MW;
- Line 2 (Bus 15 to bus 24): HVDC set-point [200, 375] is incremented in steps of 25 MW.

HVDC line 1 can be controlled to its full capacity between -100 MW and 500 MW, whereas HVDC line 2 can be controlled partially maybe due to market restrictions, so therefore, HVDC line 1 can offer more options to the TSOs to withstand the uncertainties in load.

5.3.3.2 Results and reflection

For the following evaluation, we perform 25 × 8 = 200 MC simulations to quantify the system risk associated with the coordination of two HVDC set-points. If the HVAC transfer from buses 15 to 24 was 275 MW in the single HVDC case, i.e., between buses 23 and 12; replacing the HVAC by HVDC line on left part of the system did the system good as TSOs can now steer to more green areas, and have more options to stress the system away from risky situations, see Figure 5.18. Much lower risk is observed when the set-point for HVDC line 1 are set in the range [375, 475 MW], and the set-point for HVDC line 2 are set in the range [300, 375 MW]. That means, HVDC lines can serve as a tool to shift generation.

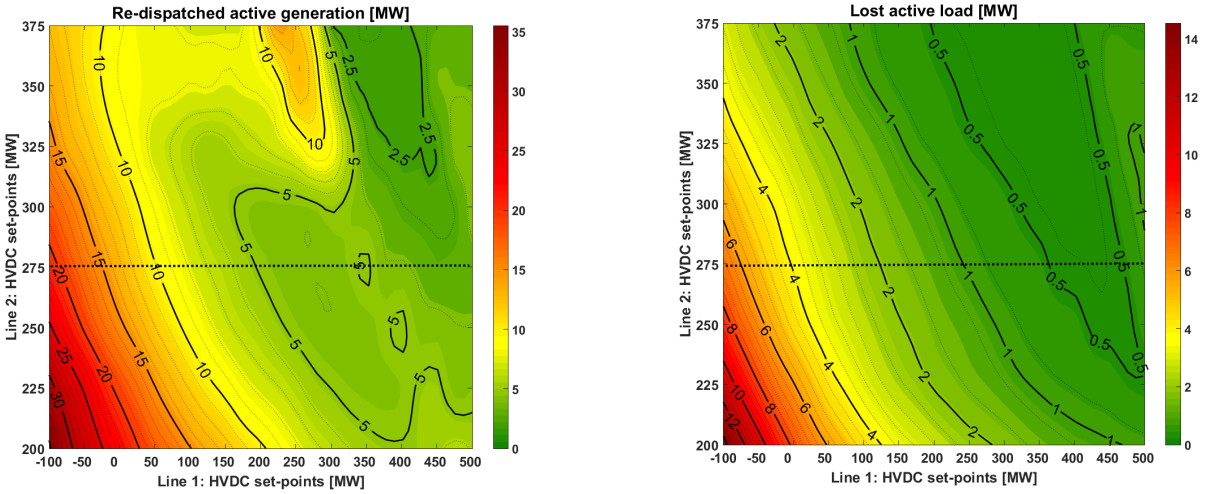

Figure 5.18: Risk in terms of re-dispatch active load and lost active load.

Figure 5.19 illustrates that the ratio of cost and risk can perhaps help TSOs to to identify / determine the "optimal" set-point. As it can be seen that the best "optimal" set-points that balances both generation dispatch costs and risk are indicated by green areas. By applying these set-points the operating point of the system moves to the most "optimal" set-point which comes with the best compromise between cost and risk. The coordination of two HVDC set-points offers more options to TSOs to steer the system away from serious problems, and if not coordinated, we may end up in risky system states. Thus, smart transmission can also have a negative impact affect on the system operational security.

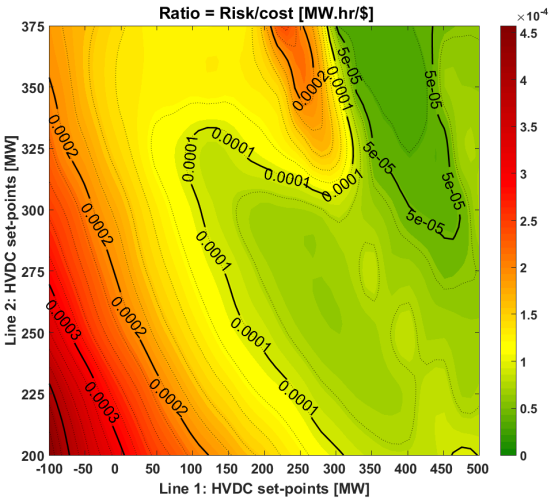

Figure 5.19: Ratio of cost and risk.

Chapter 6

Conclusions and future research

In this chapter, the main findings and conclusions are presented, followed by recommendations for follow up research work.

6.1 Summary

This thesis proposed the operational strategies for HVDC transmission in smart grid by addressing the security versus markets dilemma. Chapter 2 laid the foundation to understand the smart grid operation, and power flow modeling, necessary to investigate the power system security in the daily operational planning. Chapter 3 described the proposed RBSA methodology used to access the stochastic nature of system in-feeds. Chapter 4 discussed the current practices used by TSOs concerning day-ahead HVDC grid operation. The steady-state VSC- HVDC transmission that has been modelled in MATPOWER is described in detail. Chapter 5 proposed the need to forecast the risk associated with HVDC set-point that comes with a provided market dispatch inherent to day-ahead operation. It is observed that there is a perceived trade-off between costs and security. It was found that the coordination of the smart transmission plays an important role to lower risky system states.

6.2 Conclusions

The main conclusions can be summarized as follows:

- **Proposed RBSA methodology can be used to determine "best" HVDC set-point:** For assessing the power system security, it is proposed that TSOs should employ the proposed RBSA methodology to determine the best HVDC set-point when it is subjected to the unavoidable uncertainty of inputs (fluctuations in load and RES) inherent to day-ahead forecasting. It was shown that: i) without proper adaptability of the HVDC set-point, i.e., HVDC operated at a single, precomputed set-point, not taking into account forecast uncertainty, we could run into severe problems that can result in unnecessary high risk, and ii) with proper adaptability of the HVDC set-point, i.e., HVDC operated using a varying set of set-points, we could help to improve system security under possible uncertainties. Given a specific scenario, it was shown that HVDC set-point may improve capacity, security and efficiency of the grid (in terms of money). Moreover, TSOs cannot always use the cost optimal HVDC set-point computed by the market as there may be cases where the system can run into serious problems, e.g., cascading events or even blackouts;

- **HVDC as a part of remedial curative measure:** In order to alleviate the expected risk in day-ahead security assessment, the adaptability of HVDC set-points as a part of remedial curative measure was proposed. As HVDC have the lowest overall cost, the HVDC set-point should be able to adapt, and further more serious and more costly remedial actions such as active re-dispatch and load shedding can be avoided.
- **Coordination of HVDC set-points:** A study with two HVDC transmission lines shows how the set-points of the two HVDC transmission lines must be set by TSOs in order to find the most optimum risk vs. cost operating set-points. Two HVDC lines allow to reduce stress on one side of the system as the HVDC lines serve as a tool to shift generation. It more or less has the same effect as using a different generation shift key (GSK). Varying two HVDC set-points at the same time gives more options (degrees of freedom) to TSOs to steer the system away from risk.

6.3 Future research

The recommendations for the follow-up research can be summarized as follows:

- The proposed RBSA methodology based on the combination of MC sampling and full AC PF demand significantly complex computational resources. In order to save the computational time, we ran a MC simulation with 5.000 samples for all the case studies. However, in certain cases higher accuracy may be demanded, which could require in the order of 100.000 or even 1 million MC samples. In order to be still able to perform the risk analysis on time, one has several options: i) more hardware resources: as MC is easy to parallelize, one can simply divide the entire set of MC samples as well as the different grid points used for 1D and 2D studies over multiple computers. TSOs typically own a big cluster of computing nodes, so the proposed RBSA method can readily be used by them, ii) speed up the computations by more efficient algorithms (faster solvers), more efficient implementation and different programming language (e.g., C instead of Matlab), and iii) variance reduction techniques can be used to reduce the required number of MC samples to obtain a predefined level of accuracy;
- HVDC set-point in RBSA algorithm is set to a single value, and does not adapt during the real-time framework. However, it would be worthwhile to implement HVDC set-point adaptability during load balancing in order to steer the system away from cascading events. In this way, the HVDC set-point can automatically be adjusted by the RBSA algorithm, and TSO can adapt the set-point on a real-time framework;
- Market designs such as central dispatch, and self-dispatch markets can be evaluated based on the curative remedial actions. As the HVDC set-point in this study can be adjusted by TSOs as being part of curative remedial actions avoiding more costly remedial actions including re-dispatch, and lost active load, therefore the effect on market designs can shed more light on the overall costs of the entire system;
- It would be interesting to analyze how the optimal placement of an HVDC transmission line can affect the overall system risk, or risk in adjacent areas. This can be simulated by generating critical snapshots, by looking at different combinations of load and RES: i) high load - min RES, ii) high RES - min load, iii) high RES on one side, and iv) combination of the above. For each of these snapshots appropriate dispatch for conventional generation (CG) by solving a default AC OPF cost problem can be computed. Finally, the risk for different HVDC systems, i.e., different placement / different capacity of the HVDC transmission line can be then evaluated.

Appendix A

System parameters

A.1 Bus parameters

Table A.1: Bus parameters.

Bus	Type	P*load* (MW)	Q*load* (MVAr)	baseKV (kV)	Zone	Vmin (p.u.)	Vmax (p.u.)
1	2	108	22	138	1	1.05	0.95
2	2	97	20	138	1	1.05	0.95
3	1	180	37	138	1	1.05	0.95
4	1	74	15	138	1	1.05	0.95
5	1	71	14	138	1	1.05	0.95
6	1	136	28	138	1	1.05	0.95
7	2	125	25	138	1	1.05	0.95
8	1	171	35	138	1	1.05	0.95
9	1	175	36	138	1	1.05	0.95
10	1	195	40	138	1	1.05	0.95
11	1	-	-	230	2	1.05	0.95
12	1	-	-	230	2	1.05	0.95
13	3	265	54	230	2	1.05	0.95
14	2	194	39	230	2	1.05	0.95
15	2	317	64	230	2	1.05	0.95
16	2	100	20	230	2	1.05	0.95
17	1	-	-	230	2	1.05	0.95
18	2	333	68	230	2	1.05	0.95
19	1	181	37	230	2	1.05	0.95
20	1	128	26	230	2	1.05	0.95
21	2	-	-	230	2	1.05	0.95
22	2	-	-	230	2	1.05	0.95
23	2	-	-	230	2	1.05	0.95
24	1	-	-	230	2	1.05	0.95

A.2 Generator parameters

Table A.2: Generator parameters.

Bus	Unit	P*gen* (MW)	Q*gen* (MVAr)	Voltage (p.u.)	P*max* (MW)	P*min* (MW)
1	1	10	0	1.035	20	16
1	2	10	0	1.035	20	16
1	3	76	0	1.035	76	15.2
1	4	76	0	1.035	76	15.2
2	1	10	0	1.035	20	16
2	2	10	0	1.035	20	16
2	3	76	0	1.035	76	15.2
2	4	76	0	1.035	76	15.2
7	1	80	0	1.025	100	25
7	2	80	0	1.025	100	25
7	3	80	0	1.025	100	25
13	1	95.1	0	1.02	197	69
13	2	95.1	0	1.02	197	69
13	3	95.1	0	1.02	197	69
14	1	0	35.3	1.014	0	0
15	1	12	0	1.014	12	2.4
15	2	12	0	1.014	12	2.4
15	3	12	0	1.014	12	2.4
15	4	12	0	1.014	12	2.4
15	5	12	0	1.014	12	2.4
15	6	155	0	1.014	155	54.3
16	1	155	0	1.017	155	54.3
18	1	400	0	1.05	400	100
21	1	400	0	1.05	400	100
22	1	50	0	1.05	50	10
22	2	50	0	1.05	50	10
22	3	50	0	1.05	50	10
22	4	50	0	1.05	50	10
22	5	50	0	1.05	50	10
22	6	50	0	1.05	50	10
23	1	155	0	1.05	155	54.3
23	2	155	0	1.05	155	54.3
23	3	350	0	1.05	350	140

A.3 Transmission line parameters

Table A.3: Transmission line parameters.

Circuits	From bus	To bus	Transmission distance (miles)	Resistance (p.u.)	Reactance (p.u.)	Susceptance (p.u.)	Rating (MVA)
1	1	2	3	0.0026	0.0139	0.4611	175
2	1	3	55	0.0546	0.0211	0.0572	175
3	1	5	22	0.0218	0.0845	0.0229	175
4	2	4	33	0.0328	0.1267	0.0343	175
5	2	6	50	0.0497	0.1920	0.0520	175
6	3	9	31	0.0308	0.119	0.0322	175
7	3	24	0	0.0023	0.0839	-	400
8	4	9	27	0.0268	0.1037	0.0281	175
9	5	10	23	0.0228	0.0883	0.0239	175
10	6	10	16	0.0139	0.0605	2.4590	175
11	7	8	16	0.0159	0.0614	0.0166	175
12	8	9	43	0.0427	0.1651	0.0447	175
13	8	10	43	0.0427	0.1651	0.0447	175
14	9	11	0	0.0023	0.0839	-	400
15	9	12	0	0.0023	0.0839	-	400
16	10	11	0	0.0023	0.0839	-	400
17	10	12	0	0.0023	0.0839	-	400
18	11	13	33	0.0061	0.0476	0.0999	500
19	11	14	29	0.0054	0.0418	0.0879	500
20	12	13	33	0.0061	0.0476	0.0999	500
21	12	23	67	0.0124	0.0966	0.2030	500
22	13	23	60	0.0111	0.0865	0.1818	500
23	14	16	27	0.0050	0.0389	0.0818	500
24	15	16	12	0.0022	0.0173	0.0364	500
25	15	21	34	0.0063	0.0490	0.1030	500
26	15	21	34	0.0063	0.0490	0.1030	500
27	15	24	36	0.0067	0.0519	0.1091	500
28	16	17	18	0.0033	0.0259	0.0545	500
29	16	19	16	0.0030	0.0231	0.0485	500
30	17	18	10	0.0018	0.0144	0.0303	500
31	17	22	73	0.0135	0.1053	0.2212	500
32	18	21	18	0.0033	0.0259	0.0545	500
33	18	21	18	0.0033	0.0259	0.0545	500
34	19	20	27.5	0.0051	0.0396	0.0833	500
35	19	20	27.5	0.0051	0.0396	0.0833	500
36	20	23	15	0.0028	0.0216	0.0455	500
37	20	23	15	0.0028	0.0216	0.0455	500
38	21	22	47	0.0087	0.0678	0.1424	500

A.4 Generation cost parameters

Table A.4: Generation cost parameters.

Bus	Startup cost ($)	Shutdown cost ($)	Cost function (c2)	Cost function (c1)	Cost function (c0)
1	1500	0	0	130	400.6849
1	1500	0	0	130	400.6849
1	1500	0	0.01414	16.0811	212.3076
1	1500	0	0.01414	16.0811	212.3076
2	1500	0	0	130	400.6849
2	1500	0	0	130	400.6849
2	1500	0	0.01414	16.0811	212.3076
2	1500	0	0.01414	16.0811	212.3076
7	1500	0	0.052672	43.6615	781.521
7	1500	0	0.052672	43.6615	781.521
7	1500	0	0.052672	43.6615	781.521
13	1500	0	0.00717	48.5804	832.7575
13	1500	0	0.00717	48.5804	832.7575
13	1500	0	0.00717	48.5804	832.7575
15	1500	0	0.32841	56.564	86.3852
15	1500	0	0.32841	56.564	86.3852
15	1500	0	0.32841	56.564	86.3852
15	1500	0	0.32841	56.564	86.3852
15	1500	0	0.32841	56.564	86.3852
15	1500	0	0.008342	12.3883	382.2391
16	1500	0	0.008342	12.3883	382.2391
18	1500	0	0.000213	4.4231	395.3749
21	1500	0	0.000213	4.4231	395.3749
22	1500	0	0	0.001	0.001
22	1500	0	0	0.001	0.001
22	1500	0	0	0.001	0.001
22	1500	0	0	0.001	0.001
22	1500	0	0	0.001	0.001
22	1500	0	0	0.001	0.001
23	1500	0	0.008342	12.3883	382.2391
23	1500	0	0.008342	12.3883	382.2391
23	1500	0	0.004895	11.8495	665.1094

A.5 HVDC line specifications

Table A.5: HVDC line specifications.

HVDC line capacity [MW]	500
HVDC transfer in base case [MW]	500
Maximum reactive power at converter sending end [MVAr]	250
Minimum reactive power at converter sending end [MVAr]	-250
Maximum reactive power at converter receiver end [MVAr]	250
Minimum reactive power at converter receiver end [MVAr]	-250
Voltage at converter receiver end [p.u.]	1
Voltage at converter sending end [p.u]	1
Constant losses [MW]	11
Linear losses coefficient [MW]	0
HVDC power received at other end of line [MW]	489

Appendix B

Visualization tool

B.1 Detailed analysis when HVDC set-point is set to 325 MW

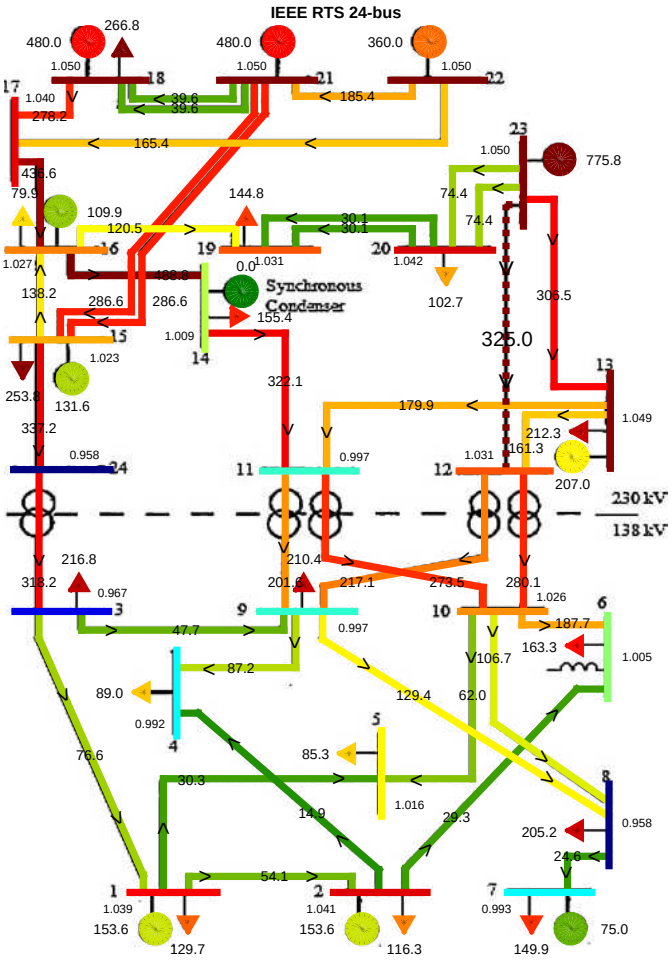

Figure B.1: Network parameters when HVDC set-point is set to 325 MW.

B.2 Detailed analysis HVDC set-point is set to 500 MW

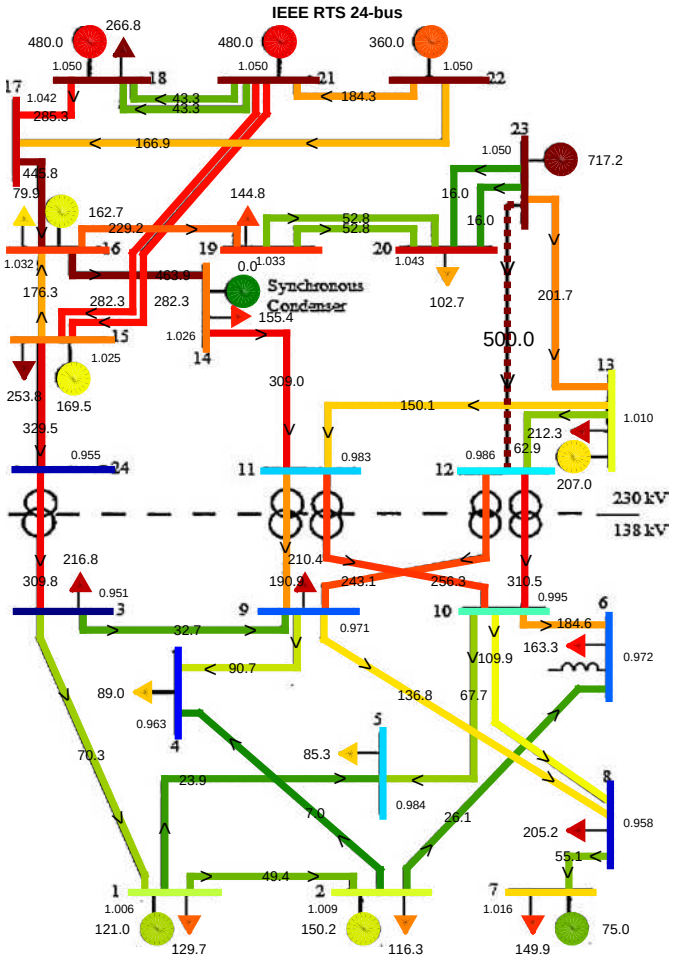

Figure B.2: Network parameters when HVDC set-point is set to 500 MW.

Bibliography

[1] E. Commission, *COM(2010) 639 final: Energy 2020: A strategy for competitive, sustainable and secure energy,* (2010).

[2] G. Papaefthymiou and K. Dragoon, *Towards 100% renewable energy systems: Uncapping power system flexibility,* Energy Policy **92**, 69 (2016).

[3] J. McCalley, *Security assessment: decision support tools for power system operators,* (2000).

[4] C. V. Fabien Roques, *Options for the future of power system regional coordination,* (2016).

[5] A. L'Abbate, G. Migliavacca, U. Hager, C. Rehtanz, S. Ruberg, H. Ferreira, G. Fulli, and A. Purvins, *The role of facts and HVDC in the future paneuropean transmission system development,* in *AC and DC Power Transmission, 2010. ACDC. 9th IET International Conference on* (IET, 2010) pp. 1–8.

[6] P. Buijs, D. Bekaert, S. Cole, D. Van Hertem, and R. Belmans, *Transmission investment problems in Europe: Going beyond standard solutions,* Energy Policy **39**, 1794 (2011).

[7] E. Commission, *Renewable energies in the 21st century: building a more sustainable future,* (2007).

[8] E. Commission, *Energy Roadmap 2050 – Impact assessment and scenario analysis,* (2011).

[9] Entso-e, *Press release: Flow-Based methodology for CWE market coupling successfully launched,* (2015).

[10] J. van Leeuwen, *A scenario-based voltage stability analysis for external constraints in flow-based capacity calculation,* (Master thesis).

[11] D. Van Hertem and M. Ghandhari, *Multi-terminal VSC HVDC for the European supergrid: Obstacles,* Renewable and sustainable energy reviews **14**, 3156 (2010).

[12] M. O. Dessouky, *The environmental impact of large scale solar energy projects on the MENA deserts: Best practices for the DESERTEC initiative,* in *EUROCON, 2013 IEEE* (IEEE, 2013) pp. 784–788.

[13] J. M. Birkebæk, A. Jäderström, R. Paprocki, and O. Ziemann, *Using HVDC Links to cope with Congestions in Neighbouring AC Networks,* PSCC, Stockholm (2011).

[14] P. L. Francos, S. S. Verdugo, H. F. Álvarez, S. Guyomarch, and J. Loncle, *INELFE—Europe's first integrated onshore HVDC interconnection,* in *Power and Energy Society General Meeting, 2012 IEEE* (IEEE, 2012) pp. 1–8.

[15] U. Project, FP7, *Deliverable 1.3: Final Report,* Tech. Rep. (2016).

[16] i. Project, *Deliverable 9.2: Project Final Report,* (2016).

[17] P. Kundur, J. Paserba, V. Ajjarapu, G. Andersson, A. Bose, C. Canizares, N. Hatziargyriou, D. Hill, A. Stankovic, C. Taylor, *et al.*, *Definition and classification of power system stability IEEE/CIGRE joint task force on stability terms and definitions,* IEEE transactions on Power Systems **19**, 1387 (2004).

[18] Z. Liu, L. van der Sluis, W. Winter, H. Paeschke, R. Becker, C. Weber, J. Eickmann, C. Schroeders, F. Oldewurtel, L. Roald, *et al.*, *Challenges, experiences and possible solutions in transmission system operation with large wind integration,* in *11th International Workshop on Large-Scale Integration of Wind Power into Power Systems* (11th International Workshop on Large-Scale Integration of Wind Power into Power Systems, 2012).

[19] Entso-e, *P5 – Policy 5: Emergency Operations,* (2015).

[20] J. McCalley, S. Asgarpoor, L. Bertling, R. Billinion, H. Chao, J. Chen, J. Endrenyi, R. Fletcher, A. Ford, C. Grigg, *et al.*, *Probabilistic security assessment for power system operations,* in *Power Engineering Society General Meeting, 2004. IEEE* (IEEE, 2004) pp. 212–220.

[21] J. D. McCalley, V. Vittal, and N. Abi-Samra, *An overview of risk based security assessment,* in *Power Engineering Society Summer Meeting, 1999. IEEE*, Vol. 1 (IEEE, 1999) pp. 173–178.

[22] Umbrella, *Deliverable D 4.1 - Risk-based assessment concepts for system security – State-of-the-art review and concept extensions,* (2012).

[23] K. Habur and D. O'Leary, *FACTS-flexible alternating current transmission systems: for cost effective and reliable transmission of electrical energy,* Siemens-World Bank document–Final Draft Report, Erlangen (2004).

[24] K. Meah and S. Ula, *Comparative evaluation of HVDC and HVAC transmission systems,* in *Power Engineering Society General Meeting, 2007. IEEE* (IEEE, 2007) pp. 1–5.

[25] C. J. Wallnerström, Y. Huang, and L. Söder, *Impact from dynamic line rating on wind power integration,* IEEE Transactions on Smart Grid **6**, 343 (2015).

[26] A. D. Little, *Untapped multi-billion market for grid companies, aggregators, utilities and industrials?* (2016).

[27] J. J. Grainger and W. D. Stevenson, *Power system analysis* (McGraw-Hill, 1994).

[28] R. D. Zimmerman, C. E. Murillo-Sánchez, and R. J. Thomas, *MATPOWER: Steady-state operations, planning, and analysis tools for power systems research and education,* IEEE Transactions on power systems **26**, 12 (2011).

[29] F. Capitanescu, J. M. Ramos, P. Panciatici, D. Kirschen, A. M. Marcolini, L. Platbrood, and L. Wehenkel, *State-of-the-art, challenges, and future trends in security constrained optimal power flow,* Electric Power Systems Research **81**, 1731 (2011).

[30] U. E. F. project, *Deliverable D3.1: Report on deterministic algorithms for EOPF,* (2013).

[31] L. Castaing, M.-S. Debry, G. Bareux, and O. Beck, *Optimal operation of HVDC links embedded in an AC network,* in *PowerTech (POWERTECH), 2013 IEEE Grenoble* (IEEE, 2013) pp. 1–6.

[32] W. Wang and M. Barnes, *Power flow algorithms for multi-terminal VSC-HVDC with droop control,* IEEE Transactions on Power Systems **29**, 1721 (2014).

[33] J. Cao, W. Du, H. F. Wang, and S. Bu, *Minimization of transmission loss in meshed AC/DC grids with VSC-MTDC networks,* IEEE Transactions on Power Systems **28**, 3047 (2013).

[34] E. Iggland, R. Wiget, S. Chatzivasileiadis, and G. Anderson, *Multi-area DC-OPF for HVAC and HVDC grids,* IEEE Transactions on Power Systems **30**, 2450 (2015).

[35] M. de Jong, G. Papaefthymiou, D. Lahaye, C. Vuik, and L. van der Sluis, *Impact of correlated infeeds on risk-based power system security assessment,* in *Power Systems Computation Conference* (Wroclaw, Poland, 2014).

[36] M. de Jong, G. Papaefthymiou, and P. Palensky, *A framework for incorporation of infeed uncertainty in power system risk-based security assessment,* IEEE Transactions on Power Systems (2017).

[37] G. Papaefthymiou, J. Verboomen, and L. van der Sluis, *Estimation of power system variability due to wind power* (IEEE, 2007).

[38] G. Papaefthymiou, P. Schavemaker, L. Van der Sluis, W. Kling, D. Kurowicka, and R. Cooke, *Integration of stochastic generation in power systems,* International Journal of Electrical Power & Energy Systems **28**, 655 (2006).

[39] M. Sklar, *Fonctions de répartition à n dimensions et leurs marges* (Université Paris 8, 1959).

[40] M. Ni, J. D. McCalley, V. Vittal, and T. Tayyib, *Online risk-based security assessment,* IEEE Transactions on Power Systems **18**, 258 (2003).

[41] M. A. Rios, D. S. Kirschen, D. Jayaweera, D. P. Nedic, and R. N. Allan, *Value of security: modeling time-dependent phenomena and weather conditions,* IEEE Transactions on Power Systems **17**, 543 (2002).

[42] G. Papaefthymiou and D. Kurowicka, *Using copulas for modeling stochastic dependence in power system uncertainty analysis,* IEEE Transactions on Power Systems **24**, 40 (2009).

[43] G. Papaefthymiou and P. Pinson, *Modeling of spatial dependence in wind power forecast uncertainty,* in *Probabilistic Methods Applied to Power Systems, 2008. PMAPS'08. Proceedings of the 10th International Conference on* (IEEE, 2008) pp. 1–9.

[44] F. Gonzalez-Longatt, C. Carmona-Delgado, J. Riquelme, M. Burgos, and J. L. Rueda, *Risk-based DC security assessment for future DC-independent system operator,* in *Energy Economics and Environment (ICEEE), 2015 International Conference on* (IEEE, 2015) pp. 1–8.

[45] X. Li, X. Zhang, L. Wu, P. Lu, and S. Zhang, *Transmission line overload risk assessment for power systems with wind and load-power generation correlation,* IEEE Transactions on Smart Grid **6**, 1233 (2015).

[46] P. Pourbeik, B. Chakrabarti, T. George, J. Haddow, H. Illian, R. Nighot, *et al.*, *Review of the current status of tools and techniques for risk-based and probabilistic planning in power systems,* CIGRE (2010).

[47] R. H. Renner and D. Van Hertem, *Ancillary services in electric power systems with HVDC grids,* IET Generation, Transmission & Distribution **9**, 1179 (2015).

[48] J. Beerten, D. Van Hertem, and R. Belmans, *VSC MTDC systems with a distributed DC voltage control-A power flow approach,* in *PowerTech, 2011 IEEE Trondheim* (IEEE, 2011) pp. 1–6.

[49] J. Beerten and R. Belmans, *Development of an open source power flow software for high voltage direct current grids and hybrid AC/DC systems: MATACDC,* IET Generation, Transmission & Distribution **9**, 966 (2015).

[50] L. Roald, S. Misra, T. Krause, and G. Andersson, *Corrective Control to Handle Forecast Uncertainty: A Chance Constrained Optimal Power Flow,* IEEE Transactions on Power Systems (2016).

[51] S. Wang, J. Zhu, L. Trinh, and J. Pan, *Economic assessment of HVDC project in deregulated energy markets,* (in Proc. 3rd Int. Conf. Electric Utility Deregulation and Restructuring and Power Technologies, Nanjing, China, Apr. 2008).

[52] S. De Boeck and D. Van Hertem, *Coordination of multiple HVDC links in power systems during alert and emergency situations,* in *PowerTech (POWERTECH), 2013 IEEE Grenoble* (June 2013) pp. 1–6.

[53] Entso-e, *HVDC Link Implementation Guide,* (2016).

[54] Entso-e, *System Operation Agreement,* (2016).

[55] Entso-e, *ENTSO-E Draft Network Code on High Voltage Direct Current Connections and DC-connected Power Park Modules,* , 1 (2014).

[56] A.-K. Marten, F. Sass, T. Krause, and D. Westermann, *Fast local converter set point adaption after AC grid disturbances based on a priori optimization,* Cigré International Symposium Across Borders – HVDC Systems and Markets Integration (2015).

[57] Entso-e, *Principles for Determining the Transfer Capacities in the Nordic Power Market,* (2016).

[58] A. Pizano-Martinez, C. R. Fuerte-Esquivel, H. Ambriz-Perez, and E. Acha, *Modeling of VSC-based HVDC systems for a Newton-Raphson OPF algorithm,* IEEE Transactions on Power Systems **22**, 1794 (2007).

[59] P. Haugland, *It's time to connect: Technical description of HVDC Light® technology,* (2006).

[60] M. C. Imhof, *Voltage Source Converter Based HVDC–Modelling and Coordinated Control to Enhance Power System Stability*, Ph.D. thesis (2015).

[61] S. S. Chatzivasileiadis, *Power system planning and operation methods integrating the controllability of HVDC*, Ph.D. thesis, ETH ZURICH (2013).

[62] S. Cole, *Steady-state and dynamic modelling of VSC HVDC systems for power system simulation,* Katholieke Universiteit Leuven, Leuven (2010).

[63] R. D. Zimmerman, C. E. Murillo-Sánchez, and R. J. Thomas, *MATPOWER: Steady-state operations, planning, and analysis tools for power systems research and education,* IEEE Transactions on power systems **26**, 12 (2011).

[64] W. Feng, A. Le Tuan, L. B. Tjernberg, A. Mannikoff, and A. Bergman, *A new approach for benefit evaluation of multiterminal VSC–HVDC using a proposed mixed AC/DC optimal power flow,* IEEE Transactions on Power Delivery **29**, 432 (2014).